

Ultra-low-frequency electromagnetic waves in the Earth's crust and magnetosphere

A V Guglielmi

DOI: 10.1070/PU2007v050n12ABEH006413

Contents

1. Introduction	1197
2. Seismomagnetic waves	1198
2.1 Generation mechanisms; 2.2 Comparative analysis of the mechanisms; 2.3 Seismomagnetic waves in the far wave zone; 2.4 Magnetic structure of a seismic wavefront; 2.5 Magnetic signal from an earthquake source; 2.6 Methods of detecting seismomagnetic signals	
3. Waves in the magnetosphere	1205
3.1 Equatorial plasma condensation by ion-cyclotron waves; 3.2 Acceleration of the polar wind by Alfvén waves; 3.3 Anharmonicity of Alfvén waves; 3.4 Ion-cyclotron resonator; 3.5 11-year activity variation in Pc1 waves	
4. Discussion	1212
4.1 ULF waves and earthquakes; 4.2 ULF waves of extramagnetospheric origin; 4.3 ULF waves and humans	
5. Conclusion	1214
References	1215

Abstract. Research on natural intra- and extraterrestrially produced electromagnetic waves with periods ranging from 0.2 to 600 s is reviewed. The way in which the energy of rock movements transforms into the energy of an alternating magnetic field is analyzed. Methods for detecting seismomagnetic signals against a strong background are described. In discussing the physics of ultra-low-frequency waves in the magnetosphere, the 11-year activity modulation of 1-Hz waves and ponderomotive forces affecting plasma distribution are emphasized.

1. Introduction

Ultra-low-frequency (ULF) waves are electromagnetic waves whose periods range from 0.2 to 600 s. There are many types of such waves. Some originate in interplanetary space and penetrate the Earth's magnetosphere; others are self-excited in the magnetosphere as a result of the interaction of solar wind and the geomagnetic field [1]. There are also ULF electromagnetic waves that accompany the propagation of sea waves [2] and seismic waves [3]. Finally, human activity, such as industrial processes and certain experiments, also generates electromagnetic signals in the ULF range (see, e.g., Ref. [4]).

The present review is devoted to ULF waves of natural origin. These waves are interesting in many respects. From

the practical standpoint, they are of interest to researchers because they can be used for prospecting hydrocarbon deposits [5] and for the diagnostics of the circumterrestrial medium [6]. For geophysicists, they are interesting because of their complex structure and dynamics, the diversity of correlations, and the beauty of wave shapes, which is reflected in the poetic name 'pearl waves' (sometimes 'pearl necklace' or simply 'pearls') for oscillations of the geomagnetic field in the 1-Hz range [7, 8]. Biologists and physicians are interested in ULF waves because such waves constitute one of the cosmic factors that may have an effect on the physiological activity of organisms [9, 10]. But physicists are interested in ULF waves because of their enigmatic origin (in addition to other aspects). Detecting and observing ULF waves is a source of many difficult and diversified problems. The ambiguity of the initial and boundary conditions and the inaccuracy of data on the generation mechanisms and on the conditions of propagation of such waves dictate the need to discuss not a single model of the origin and evolution of the waves but several models, and also to compare the conclusions drawn from theory and the results of observations in the best possible manner.

Earlier reviews [8, 11–14] and monographs [1, 4, 6] focused almost entirely on waves of cosmic origin. We therefore begin our discussion with a more thorough (than is customary) treatment of ULF waves, whose sources are in the Earth's crust and which are triggered by earthquakes. Such waves are called seismomagnetic. Section 2 is devoted to important problems of the physics of seismomagnetic waves. In Section 3, we discuss various aspects of the physics of magnetospheric waves. They relate to the 11-year solar-cyclic activity of the frequency of wave generation, equatorial plasma condensation, acceleration of polar winds, and the anharmonicity of standing Alfvén waves. In discussing the vexing questions and unresolved problems in Section 4, we

A V Guglielmi Schmidt Institute of Physics of the Earth,
Russian Academy of Sciences,
ul. B. Gruzinskaya 10, 123995 Moscow, Russian Federation
Tel. (7-495) 582 99 71. E-mail: guglielmi@mail.ru

Received 21 May 2007
Uspekhi Fizicheskikh Nauk 177 (12) 1257–1276 (2007)
10.3367/UFNr.0177.200712a.1257
Translated by E Yankovsky; edited by A M Semikhatov

examine the origin of a weak (but statistically reliable) 7-day modulation of the activity of ULF waves. It is assumed that the presence of such modulation is proof of a noticeable anthropogenic effect on the extraterrestrial medium. Finally, in Section 5, we briefly characterize the general state of research in this field.

2. Seismomagnetic waves

A strong pulse of a magnetic field in the ULF range is generated when a large-scale fault rupture occurs in an earthquake source. The pulse leaves the region where it was generated and travels along the Earth's surface ahead of the elastic wavefront. Under favorable conditions, it can be detected in the epicentral zone without being distorted by a seismographic disturbance [15–23]. The analysis of such signals may provide useful information about the physical processes that occur in the earthquake source. Far from the epicenter, seismic waves excite weak electromagnetic oscillations, which, however, merit close consideration [24–30]. In particular, the prospects of using seismomagnetic signals to study the electrodynamic properties of rock in natural occurrence are certainly of interest [29, 30]. We now examine the mechanisms by which the energy of rock movement is transformed into the energy of an electromagnetic field, the structure of the seismomagnetic field, and the methods of recording seismomagnetic signals against the background of noise.

2.1 Generation mechanisms

The acceleration of rock generates forces of inertia that trigger what is known as the *inertial* mechanism of generation of a variable magnetic field \mathbf{B} . The equation that describes this process has the form

$$\frac{\partial \mathbf{B}}{\partial t} = -\alpha \nabla \times \mathbf{A} + \frac{c^2}{4\pi\sigma} \nabla^2 \mathbf{B}, \quad (1)$$

where $\mathbf{A} = \partial \mathbf{V} / \partial t$ is the rock acceleration, with \mathbf{V} being the velocity, α is the coefficient of mechanomagnetic transformation, and σ is the rock conductivity. For simplicity, we assume the medium to be homogeneous in the unperturbed (undisturbed) state. We see that the vortex lines of the acceleration field $\mathbf{A}(\mathbf{x}, t)$ are the source of a seismomagnetic field. If we take the dimensions of the physical quantities in the equation into account, we can write $\alpha = m_{\text{eff}} c / e$, where m_{eff} is a certain effective mass of charge carriers, e is the elementary electric charge, and c is the speed of light. Locally, the medium is therefore fully characterized by two parameters, σ and m_{eff} .

The idea of an inertial mechanism of generating seismomagnetic signals was introduced in Refs [31–33]. Earlier, Eleman [24] mentioned the inertial mechanism but considered it insignificant when compared with other mechanisms, i.e., the induction, the piezomagnetic, and the strain mechanisms. This was a mistake, and today we can only guess that Eleman most probably had in mind the Tolman–Stuart effect in metals. As is known (see Ref. [34]), $\alpha = -m_e c / e$ in this case, where m_e is the electron mass. But in the Earth's crust, electric charge is transferred mainly by ions and not by electrons. It would, however, be a mistake to simply replace m_{eff} with m_i , the ion mass. Rock consists of porous solids whose pores are partially or completely filled with a weak solution of a strong electrolyte. As the rigid frame of rock is accelerated, the inertial mass of the charge carriers appears to increase.

According to a rough estimate [31], the additional mass is equal to the mass of the liquid filling the pores within the volume of a disk whose radius is of the order of the mean pore radius and thickness is of the order of the Debye radius (see also Refs [4, 35]). Clearly, this additional mass is much larger than the conduction-ion mass. A more exact estimate depends on the structure of the moist porous body, but in any case α in the Earth's crust is much larger than in a metallic conductor (by a factor of 10^8).

A remark concerning terminology is in order. In a number of recently published papers (e.g., see Ref. [35]), the inertial mechanism of generation is called the electrokinetic mechanism. This is not the proper name for a number of reasons. Of course, names are simply a question of agreement, but they can effectively serve as such only if they have the same meaning in different contexts, without having to repeat their definitions over and over again. For geophysicists studying the electric field of seismic waves, the term 'electrokinetic mechanism' is most commonly associated with seismoelectric signals of the second kind, discovered by Ivanov [36]. However, the electrokinetic mechanism of generation of such signals proposed by Frenkel [37] does not induce oscillations in the magnetic field. To avoid any misunderstanding, it is only natural to call it the inertial mechanism, rather than the electrokinetic mechanism of generation of a magnetic field as a result of accelerated movement of rock, as was done in the original publications [31–33].

The essence of the *induction* mechanism is that the movement of the conducting crust in the constant magnetic field of the Earth's core induces currents that generate a variable magnetic field. (In other words, the core serves as an inductor and the core as the armature, to draw an analogy with an ordinary DC generator.) The generation process is described by the equation

$$\frac{\partial \mathbf{B}}{\partial t} = \nabla \times (\mathbf{V} \times \mathbf{B}_0) + \frac{c^2}{4\pi\sigma} \nabla^2 \mathbf{B}, \quad (2)$$

where \mathbf{B}_0 is the principal electromagnetic field. Equation (2) coincides with one of the linearized equations of magnetohydrodynamics [34, 38]. We note that the first term in the right-hand side of Eqn (2) can be replaced with $(\mathbf{B}_0 \nabla) \mathbf{V} - \mathbf{B}_0 (\nabla \mathbf{V})$ because the field \mathbf{B}_0 can often be considered homogeneous when seismomagnetic phenomena are modeled.

The effect of the *piezomagnetic* mechanism of generation is related to the stresses P_{ij} in rock containing ferromagnetic inclusions, while the effect of the *strain* mechanism is caused by the modulation of telluric currents under volume strain $\theta = \nabla \mathbf{U}$, which changes the porosity of rock and, consequently, its electric conductivity. Here, $\mathbf{U}(\mathbf{x}, t)$ is the displacement field. Generally speaking, the above four mechanisms act simultaneously in an earthquake, and it therefore comes as no surprise that we must write an equation that governs generation with all the basic elements of rock mechanics — acceleration, velocity, strain, and stress — taken into account. We introduce the notation

$$\mathbf{C} = -\alpha \mathbf{A} + \mathbf{V} \times \mathbf{B}_0 + \beta \theta \mathbf{E}_0 + \nabla \times \mathbf{M}, \quad (3)$$

$$\beta = \frac{\partial \ln \sigma}{\partial \theta}, \quad M_i = (\gamma_1 P_{ii} \delta_{ij} + \gamma_2 P_{ij}) B_{0j}, \quad (4)$$

$$D = \frac{\partial}{\partial t} - \frac{c^2}{4\pi\sigma} \nabla^2, \quad (5)$$

and write the equation governing the generation in the form [33]

$$D\mathbf{B}(\mathbf{x}, t) = \nabla \times \mathbf{C}(\mathbf{x}, t). \quad (6)$$

For simplicity, we here assume that the rock conductivity σ , the parameters of mechanomagnetic transformation α , β , γ_1 , and γ_2 , and the external fields \mathbf{E}_0 and \mathbf{B}_0 are uniformly distributed in space and are time independent.

Clearly, the magnitude of the magnetic signal is proportional to the amplitude of seismic vibrations, while the relative effectiveness of the generation mechanisms depends in a complicated manner on a combination of parameters. The relevant parameters vary within broad limits and, moreover, are difficult to measure in many cases. In quantitative estimates, we use some characteristic values of the parameters, but it must be remembered that in general, interpreting seismomagnetic events correctly requires knowing the entire set of parameters in the area where the measurements are being done. We reconsider this problem in Section 4.

Obviously, Eqn (6) should be solved with a given movement of the medium. At the same time, it was not necessarily obvious that in studying seismomagnetic phenomena we can completely ignore the effect on the medium movement, not only of the field \mathbf{B} but also of the external magnetic field \mathbf{B}_0 , because if we supplement Eqn (2) with the linearized equation of motion of an ideally conducting incompressible liquid ($\sigma \rightarrow \infty$ and $\nabla \mathbf{V} = 0$), then we can derive the dispersion relation

$$\omega = c_A k_{\parallel} \quad (7)$$

that describes the propagation of Alfvén magnetohydrodynamic waves. Here, ω is the wave frequency, k_{\parallel} is the projection of the wave vector on the external magnetic field, and $c_A = (4\pi\rho)^{-1/2} B_0$ is the Alfvén velocity. But if we supplement Eqn (2) with the linearized equations of elasticity theory (with the Lorentz force taken into account), we see that magnetoelastic waves similar to Alfvén waves occur in well-conducting solids. For such waves, the dispersion relation has the form

$$\omega = \sqrt{c_A^2 k_{\parallel}^2 + c_t^2 k^2}, \quad (8)$$

where $c_t = (\mu/\rho)^{1/2}$ is the speed of transverse elastic waves and μ is the shear modulus. There was a time when it was assumed (see Ref. [39]) that taking the effect of the external magnetic field B_0 on the propagation of transverse waves into account could be important in seismology. However, the propagation of transverse waves in the Earth's crust obeys the ordinary dispersion relation $\omega = c_t k$, and hence no modification of type (8) is required because $B_0 \ll \sqrt{4\pi\mu}$ with a large margin [40]. Furthermore, this strong inequality holds for all known solids in nature, including the crust of pulsars, where B_0 is higher than in the Earth's crust by 12 to 13 orders of magnitude [41].

A remark concerning the freezing of the magnetic field in a conducting medium is in order. Sometimes, it is unjustifiably assumed (see Ref. [42]) that the freezing-in condition has the form $R \gg 1$, where R is the magnetic Reynolds number. Actually, this condition is of the form $L \gg 1$, where the Lundquist number L for the given range of problems is $L = 4\pi\sigma\omega/(ck)^2$. This alteration is important in the following sense. We recall that as a result of the action of the induction mechanism, sea waves generate very weak oscillations

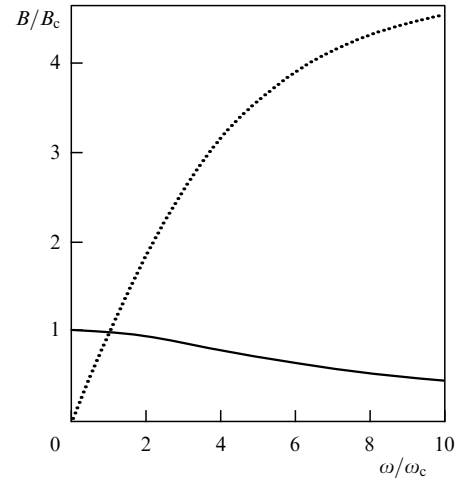


Figure 1. Frequency dependence of the amplitude of seismomagnetic oscillations. The solid and dotted curves correspond to the induction and inertial mechanisms of generation.

in a magnetic field [2, 43]. Because the amplitude of seismic waves is several orders of magnitude smaller than that of a sea wave, it would seem that there is no hope of recording the seismomagnetic signal. However, $R \ll 1$ in both cases, but $L \sim 1$ for seismic waves and $L \ll 1$ for sea waves, i.e., the Earth's crust 'pulls' at the geomagnetic field more strongly than sea water. As a result, the induction effect is enhanced so strongly that the seismomagnetic signal can, in principle, be detected [25, 40].

2.2 Comparative analysis of the mechanisms

We now use Eqns (1) and (2) to comparatively analyze the relative effectiveness of the inertial and induction mechanisms of generation of a magnetic field. We begin by specifying the velocity field $\mathbf{V}(\mathbf{x}, t)$ and assume that this field is generated by a plane elastic transverse wave $\exp(i\mathbf{k}\mathbf{x} - i\omega t)$ propagating with a speed c_t in a homogeneous infinite medium. Bearing in mind that $k = \omega/c_t$, we immediately conclude from Eqns (1) and (2) that for a given amplitude of the elastic wave, the amplitude of an inertial (induction) magnetic signal is an increasing (decreasing) continuous function of ω , with $B \rightarrow 0$ ($B \rightarrow \text{const}$) as $\omega \rightarrow 0$ and $B \rightarrow \text{const}$ ($B \rightarrow 0$) as $\omega \rightarrow \infty$. This implies that there is a critical frequency ω_c at which the two mechanisms are equally effective, with the induction mechanism dominating at low frequencies and the inertial mechanism at high frequencies. It can be easily seen that

$$\omega_c = \frac{B_{0\parallel}}{\alpha}, \quad (9)$$

where $B_{0\parallel}$ is the projection of the external magnetic field on the direction of propagation.

The critical frequency may vary within broad limits. According to Refs [35, 44], it takes values that range from several millihertz to several hertz, depending on the specific conditions. At $B_{0\parallel} = 0.2$ G, $\alpha = 0.8$ abs. units, $c_t = 3$ km s⁻¹, and $\sigma = 0.1$ S m⁻¹, the frequency ω_c amounts to 0.25 s⁻¹, and the function $B(\omega)$ has the shape depicted in Fig. 1, where B_c is the oscillation amplitude at the critical frequency. The solid and dotted curves respectively correspond to induction and inertial oscillations. Near the critical frequency, the two oscillation amplitudes are comparable, but the oscillations differ in polarization: in induction oscillations, the magnetic

field \mathbf{B} is parallel to the velocity \mathbf{V} of the medium movement, while in inertial oscillations, the magnetic field is perpendicular to the plane containing the vectors \mathbf{k} and \mathbf{V} .

Other pairs of mechanisms can be compared similarly. For this, we should find the stimulated solutions of Eqn (6) with a given medium movement and fixed boundary conditions, perform a spectral decomposition, and represent the relative effectiveness of the mechanisms by pair ratios of the spectral amplitudes. An appropriate analysis [44] that uses simple models of propagation of bulk and surface elastic waves has revealed that there exists a set of critical parameters that allows estimating the relative contribution of different mechanisms to the dependence on the wave frequency and the mechano-electromagnetic properties of the medium. These parameters can be used in interpreting signals from earthquakes and in planning explosion and seismo-vibrational experiments in exciting geoelectromagnetic fields. These critical parameters have a very large spread, but it is still possible to conclude that the inertial, induction, and piezomagnetic mechanisms are roughly equal in effectiveness, while the strain mechanism should, in our opinion, be taken into account only in a special state of rock, the so-called percolation threshold [45, 46].

2.3 Seismomagnetic waves in the far wave zone

Far from the earthquake source, the waves may be considered locally planar. This approximation has been used in a number of model problems involving the excitation of magnetic oscillations by elastic waves; the references can be found in review [3]. We discuss several typical problems without examining the cumbersome formulas that emerge in the calculations of seismomagnetic effects.

It could well be that such an approach is not rigorous enough from the standpoint of geophysics, but, on the other hand, it is always interesting to identify the limit in which only one mechanism (which is of interest to us) dominates. In this connection, it is interesting to study what is known as the Love wave model. In this model, $\theta = 0$, i.e., the strain mechanism does not operate. The other three mechanisms are present, but the induction and piezomagnetic mechanisms provide a negligible contribution to the magnetic field at the surface of a body. In other words, if we are interested in the seismomagnetic signal at the Earth's surface, it suffices to take only the inertial generation mechanism into account. (We note that deep inside a body, all three mechanisms provide comparable contributions to the magnetic field.) The same property is exhibited by the transverse wave model in the particular case where the vector \mathbf{V} is parallel to the surface of the body. We now examine the inertial magnetic effect within this second model, because it is simpler than the Love wave model.

We suppose that a homogeneous conducting body has a free surface and occupies the half-space $z \leq 0$. We take the field of the elastic transverse wave $\mathbf{V} = (0, V, 0)$ in the form [47]

$$V = V_0 \cos\left(\frac{\omega}{c_t} z \cos \phi\right) \exp[i(kx - \omega t)], \quad (10)$$

where V_0 is the wave amplitude, $k = (\omega/c_t) \sin \phi$, and ϕ is the angle of wave incidence. Substituting (10) in (1), we find \mathbf{B} inside the body. The field outside the body ($z > 0$) satisfies the equations

$$\nabla^2 \mathbf{B} = 0, \quad \nabla \mathbf{B} = 0. \quad (11)$$

Their solution combines with (10) and the condition at infinity yields

$$B_z = iB_x = B \exp[-kz + i(kx - \omega t)]. \quad (12)$$

The amplitude B can be found from the boundary condition at the body surface $z = 0$:

$$B = -\frac{\alpha V_0 \omega_\sigma \omega (\omega \sin^2 \phi - i\omega_\sigma)^{1/2} \sin \phi}{c_t (\omega - i\omega_\sigma) [(\omega \sin^2 \phi - i\omega_\sigma)^{1/2} + \omega^{1/2} \sin \phi]}, \quad (13)$$

where $\omega_\sigma = 4\pi\sigma(c_t/c)^2$. If $\omega \ll \omega_\sigma$, then

$$B \approx -i \frac{V_0}{c_t} \alpha \omega \sin \phi;$$

but if $\omega_\sigma \ll \omega \sin^2 \phi$, then

$$B \approx -\frac{V_0}{2c_t} \alpha \omega_\sigma \sin \phi.$$

For $z < 0$, the formulas for B_x and B_z are too cumbersome to be presented here.

We now return to the Love wave. Solving the general case requires using numerical methods, because the Love wave exists only in layer-inhomogeneous bodies. Methodologically, it would be wrong to account for the inhomogeneity in the depth distribution of the mechanical parameters and not to account for the inhomogeneity of the distribution of the electrodynamic parameters. Allowing for both inhomogeneities complicates the problem. But in the case of a thin, porous, and moisture-saturated film covering an elastic nonconducting body, there is an analytic solution. To be precise, the vibrations of the film initiated by a Love wave generate a magnetic field that at $z \geq 0$ has the structure as in (12), with

$$B = \alpha \omega \frac{V_0}{c_L} \left(i - \frac{c^2}{2\pi c_L \Sigma} \right)^{-1}, \quad (14)$$

where c_L is the Love wave velocity and Σ is the integrated conductivity of the film. It is assumed that the film thickness is much smaller than the characteristic size of the vertical inhomogeneity of the mechanical parameters.

In contrast to a Love wave, a Rayleigh wave propagates along the surface of a homogeneous elastic body. Knowing the solution of the mechanical problem [47], we can easily find the respective solution of the equation of magnetic-field generation in explicit form [25, 48]. Such a solution was used in Ref. [44] to interpret the magnetic signal from the exceptionally strong earthquake (magnitude $M = 8.6$) that originated in Alaska on March 24, 1964. The magnetic signal from this earthquake was registered by a helium magnetometer located at Bergen Park, Colorado at a distance of 4600 km from the epicenter [24]. Magnetic oscillations with the period 20 s and amplitude 0.2 nT began at the moment of arrival of the seismic wave. The parameters of the seismic vibrations were as follows: the maximum velocity of vertical displacement of soil was 0.7 cm s^{-1} and the maximum velocity of the horizontal displacements was 0.4 cm s^{-1} . The mode structure of the seismic vibrations is not quite clear, but it can be assumed that we are dealing with a Rayleigh wave.

Eleman [24], who discovered the magnetic signal, excluded the possibility of a simple coincidence, because the

relation of the magnetic oscillations to the seismic vibration was too obvious. According to the estimates in Ref. [24], the piezomagnetic effect was at least three times weaker than the recorded signal. The relative displacement of the non-uniformly magnetized rock in the vicinity of the observation point could not, obviously, produce the required effect. As an alternative, Eleman suggested the induction mechanism. In his analysis, he limited himself to qualitative reasoning, augmenting it by the hypothesis that there is a well-conducting layer at a certain depth near Bergen Park. But a quantitative analysis in [44] involving the solution of generation equation (2) showed that the amplitude of the induction signal does not exceed 0.1 nT, i.e., the signal is at least twice as weak as the recorded one. It is unclear whether taking the inertial mechanism into account would eliminate the discrepancy, because the electrodynamic parameters of the rock in the vicinity of the observation point are unknown. Generally, such uncertainty, which hinders interpretation of seismomagnetic data, is typical of all the events described in the literature.

2.4 Magnetic structure of a seismic wavefront

We consider a plane elastic wave with an abrupt leading front that propagates along the x axis in a homogeneous conducting medium placed in an external magnetic field $\mathbf{B}_0 = (B_{0\parallel}, 0, B_{0\perp})$. We suppose that at the instant $t = 0$, the displacement field is

$$U(x) = \begin{cases} U_0 \exp(ik_0x) & \text{for } x < 0, \\ 0 & \text{for } x \geq 0. \end{cases} \quad (15)$$

To be specific, we consider a longitudinal wave. Then the displacement vector is $\mathbf{U} = (U, 0, 0)$, with $U = U(x - c_1t)$, where c_1 is the speed of the elastic longitudinal wave. A magnetic-field perturbation $\mathbf{B} = (0, 0, B)$ is described by induction equation (2). We represent $B(x, t)$ in the form of a superposition of traveling waves,

$$B(x, t) = \int_{-\infty}^{\infty} B_k \exp[ik(x - c_1t)] dk. \quad (16)$$

It follows from Eqn (2) that B_k can be expressed in terms of the Fourier transform U_k of the displacement field as

$$B_k = \frac{kB_{\perp}U_k}{i - kd}, \quad (17)$$

where $d = c^2/4\pi\sigma c_1$ and

$$U_k = \frac{iU_0}{2\pi} \int_0^{\infty} \exp[i(k - k_0)x] dx. \quad (18)$$

Combining (16)–(18), we find that

$$B(x, t) = \frac{B_{\perp}U_0}{(k_0d - i)d} \exp[ik_0(x - c_1t)] \quad (19)$$

for $x < c_1t$ and

$$B(x, t) = \frac{B_{\perp}U_0}{(k_0d - i)d} \exp\left(-\frac{x - c_1t}{d}\right) \quad (20)$$

for $x > c_1t$.

Clearly, for $x > c_1t$, i.e., ahead of the leading elastic wavefront, a magnetic precursor moves that exponentially decreases with the distance from the wavefront [41]. The

damping constant d depends on the electric conductivity σ and the speed c_1 but is independent of the frequency $\omega_0 = c_1k_0$. Behind the wavefront ($x < c_1t$), the magnetic field oscillates with the frequency ω_0 .

Transverse waves are analyzed similarly. The result is obtained from (19) and (20) by replacing c_1 with c_t and $B_{0\perp}$ with $B_{0\parallel}$. The vector \mathbf{B} is polarized in this case in the same way as the vector \mathbf{U} . For instance, with $\mathbf{U} = (0, U, 0)$, we have $\mathbf{B} = (0, B, 0)$. In contrast to the longitudinal wave, the transverse wave also triggers the inertial mechanism, but we do not discuss this aspect here because the appearance of a precursor in no way depends on the field-generation mechanism. The effect is due solely to the motion of the wavefront.

The above model is too simple to result in meaningful predictions of effects or to allow interpreting the observations correctly. Nevertheless, we note paper [15], which describes the magnetic signal recorded in the Kamchatka region from an earthquake that occurred at a distance of 70 km with the epicenter at a depth of 80 km. The signal arrived several seconds before the seismic wavefront. However, it just may be possible that this was not the magnetic precursor of the wavefront but a pulse generated at the earthquake source. In any case, a theory that is expected to provide the correct interpretation of terrestrial observations must take the effect of the Earth's surface on the structure of the magnetic precursor into account. It turns out that after the elastic wavefront surfaces, the magnetic precursor decreases in accordance with a power law rather than an exponential law as we move away from the front along the Earth's surface [3].

2.5 Magnetic signal from an earthquake source

The maximum accelerations, velocities, displacements, and drops in mechanical strain in the Earth's crust are determined by the formation of a large-scale fault rupture and the motion of rupture edges in the earthquake source. We should expect magnetic signals of large amplitudes in this event. The problem can be formulated as follows. We select a model for the vector displacement field $\mathbf{U}(\mathbf{x}, t)$ according to our ideas about the dynamics of the earthquake source. We then seek the solution $\mathbf{B}(\mathbf{x}, t)$ of the magnetic-field generation equation with a zero initial condition and appropriately chosen boundary conditions. The standard kinematic models of rock movement in the earthquake source [49] are too complicated to even attempt to find formulas that link the theory of magnetic-field generation to the observational data. Hence, we limit ourselves to examining the magnetic pulse from the source within two idealized models, the propagating destruction model [19, 23] and the flat conformal model [18, 20].

Because Eqn (6) is linear, we can study the different generation mechanisms independently and then add the results. Comparative analysis of the effectiveness of the mechanisms shows that one of these mechanisms is predominant in some cases, while a different one is in other cases, depending on the medium parameters and the scale of movement at the source. At the same time, it is clear that the formal solution depends only weakly on the choice of the mechanism. In order not to clutter up our discussion, we focus on the inertial mechanism, which comes into play when the fluid vibrates in the pores and cracks because of forces of inertia in the vortex motion of the rock skeleton during an earthquake. We note that there was a case (about which more is to be said later) in which the inertial mechanism of magnetic-signal generation was, apparently, predominant.

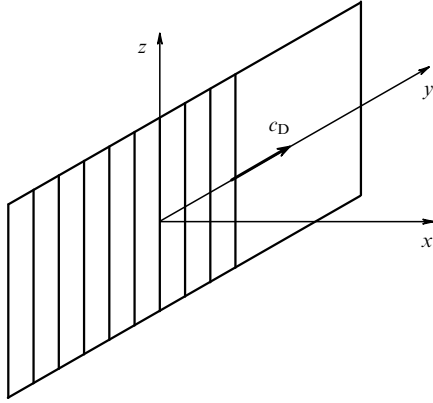


Figure 2. A model of a propagating fault rupture.

We write generation equation (1) as

$$\frac{\partial}{\partial t}(\mathbf{B} + \alpha\mathbf{\Omega}) = \frac{c^2}{4\pi\sigma} \nabla^2 \mathbf{B}, \quad (21)$$

where $\mathbf{\Omega} = \nabla \times \mathbf{V}$ and $\mathbf{V} = \partial \mathbf{U} / \partial t$, and suppose that the destruction propagates in only one direction, as was the case, for instance, in the Chilean earthquake of May 22, 1960, where the destruction front moved from north to south with the speed $3\text{--}4 \text{ km s}^{-1}$ over a distance of approximately 1000 km. To illustrate how the inertial mechanism operates, we consider the Knopov – Hilbert model

$$U(x, y, t) = -U_m H\left(t - \frac{y}{c_D}\right) \text{sgn } x, \quad (22)$$

which describes inelastic motion in the source in the simplest possible way (‘a moving Heaviside dislocation’; see Ref. [49]). Here, the x axis is perpendicular to the fault plane, U is the y -component of \mathbf{U} (the displacement vector), H is the Heaviside function, and c_D is the speed with which the destruction propagates, which is close to the speed c_t of transverse waves (Fig. 2). Then $\mathbf{\Omega} = (0, 0, \Omega)$, where

$$\Omega = -2U_m \delta(x) \delta\left(t - \frac{y}{c_D}\right), \quad (23)$$

i.e., we have a vortex filament with a constant vorticity $\mathbf{\Omega}$ moving with a constant speed c_D in the direction perpendicular to the filament along the fault plane and generating a magnetic field. The corresponding solution of Eqn (21) that decreases at infinity has the form $\mathbf{B} = (0, 0, B)$, where

$$B(x, y, t) = \frac{\alpha c_D^3 U_m}{2\pi\chi^2} \left\{ K_0\left(\frac{rc_D}{2\chi}\right) + \left(\frac{y - tc_D}{r}\right) K_1\left(\frac{rc_D}{2\chi}\right) \right\} \times \exp\left[-\frac{c_D}{2\chi}(y - tc_D)\right]. \quad (24)$$

Here, $r = [x^2 + (y - c_D t)^2]^{1/2}$, $\chi = c^2/4\pi\sigma$, and U_m is the displacement of the rupture edges (it is half of what is known as the strike shift). Clearly, the field is transferred as a whole, together with the destruction front. Figure 3 shows the curves of constant magnetic field strength at time $t = 0$. The shape of the magnetic signals is shown in Fig. 4. (Here, we used dimensionless units for the spatial coordinates and the magnetic field strength.)

Not often does one encounter sources of such enormous dimensions as in the Chilean earthquake. In the case of

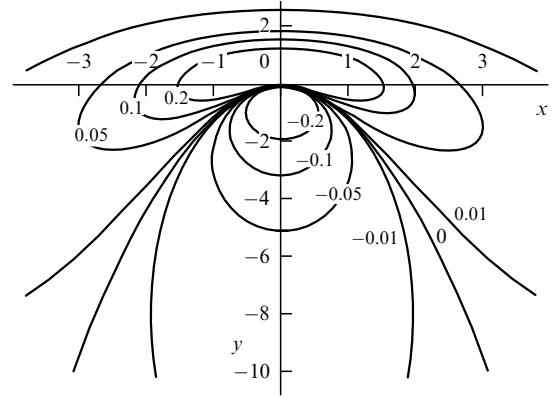


Figure 3. Curves of constant magnetic field strength in the x, y plane.

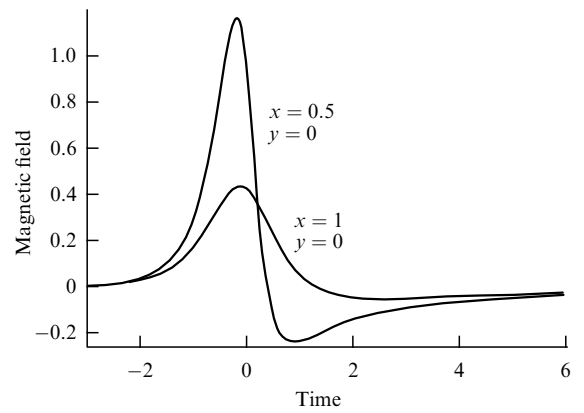


Figure 4. Magnetic pulses at distances $x = 0.5$ and $x = 1.0$ from the fault rupture plane (relative units).

seismic sources of moderate or small dimensions, the nonuniformity of fault rupture movement must be taken into account in general. It must also be remembered that the propagation of destruction is unlikely to be unidirectional. The complications associated with the nonuniformity of movement and the nontrivial configuration of the destruction front are usually ignored and the common approach here is to use the so-called flat conformal model in interpreting seismomagnetic data.

We suppose that at the instant $t = 0$, the rupture occurs simultaneously along the plane $x = 0$, with its edges shifting in opposite directions parallel to the y axis. We set $U(x, t) = -U_m \theta(t) \text{sgn } x$. Here, the effect of destruction propagation is taken into account implicitly by selecting an appropriate source time function $\theta(t)$. Equation (21) becomes

$$\frac{\partial B}{\partial t} = \chi \frac{\partial^2 B}{\partial x^2} + 2\alpha U_m \frac{\partial^2 \theta}{\partial t^2} \delta(x). \quad (25)$$

Its solution can be written as an integral:

$$B(x, t) = \frac{\alpha U_m}{\sqrt{\pi\chi}} \int_0^t \exp\left[-\frac{x^2}{4\chi(t-\tau)}\right] \frac{d^2 \theta}{d\tau^2} \frac{d\tau}{\sqrt{t-\tau}}. \quad (26)$$

It remains to choose the source time function. If we use the Brune model [50]

$$\theta(t) = \left[1 - \exp\left(-\frac{t}{T}\right)\right] H(t), \quad (27)$$

where T is the characteristic time of mechanical motion, then it follows from (26) that at the initial instant, the field is, so to say, buried in the fault, which is understandable because the current generated at that instant forms a kind of flat, infinite solenoid. As time passes, the field emerges from the source and diffuses into the surrounding space.

Using (26) and (27), we can calculate the magnetic moment of a unit of fault plane, $m = \alpha U_m / 2\pi T$, and estimate the total magnetic moment of a real source with finite dimensions, $M = mS$, where S is the fault area. Seismologists have established a number of empirical relations between the source parameter S , T , and U_m , on the one hand, and the earthquake magnitude M on the other [16, 49, 51, 52]. This allows expressing the magnetic moment M in terms of the earthquake magnitude M . For $M \geq 5$, we have

$$M = \alpha 10^{pM+q}, \quad (28)$$

where $p = 1.385$ and $q = 5.65$ if M and α are expressed in absolute units.

We use estimate (28) to interpret the unipolar magnetic pulse from a strong earthquake that occurred in Japan. The observations were done in the standby mode by the advanced interval method [21], i.e., the signal was sought in the short time interval after the beginning of the earthquake but before the seismic wavefront arrived (see Section 2.6). An earthquake with the magnitude $M = 7.2$ occurred on January 1, 1995 at the depth 17 km. A unipolar magnetic signal with the amplitude $B = 0.6$ nT was recorded by a three-component magnetometer at Mineyama station located northeast of the epicenter at the distance $r = 100$ km. The experimenters, Iyemori et al. [21], discussed the possibility of interpreting the magnetic signal as the result of the induction generation mechanism operating in the source. Using seismological data, they specified the geometry and kinematics of the seismic source and found that electromagnetic induction generates a signal with the amplitude about 0.03 nT, which strongly contradicts the observed facts. At the same time, the hypothesis that the inertial mechanism operates in the source leads to estimates of the magnetic pulse amplitude that are in reasonable agreement with the results of observation [22, 23]. Indeed, for $M = 7.2$ and $r = 100$ km, we have $B \approx M/r^3 \approx 0.6$ nT for a fairly moderate value of the mechanomagnetic transformation coefficient, $\alpha = 1.4$ abs. units.

2.6 Methods of detecting seismomagnetic signals

One of the goals of seismoelectrodynamics is to detect seismomagnetic signals, i.e., electromagnetic oscillations excited in the Earth's crust by seismic waves and other types of mechanical movement of rock, i.e., the movement of rupture edges during the formation of large-scale fault ruptures in the earthquake source. This is not easy because the observations are hindered by noise. A typical seismographic interference is the parasitic signal induced by the principal geomagnetic field in the magnetometer sensors that are in oscillatory motion initiated by the seismic wave. In some cases, observations are hindered by the microphone effect, i.e., a parasitic signal generated by relative movements of the elements of the measuring device. Industrial noise and magnetospheric ULF oscillations that reach the Earth's surface are also disturbances. The presence of strong disturbances makes gathering experimental data difficult and complicates the verification of ideas concerning the

mechano-electromagnetic transformations in the Earth's crust.

Eleman [24] thoroughly analyzed the reaction of magnetic instruments to seismic vibrations and concluded that the simplest way to suppress seismographic noise is to use the method of modular measurements with a quantum magnetometer. The method was successfully used to record magnetic oscillations with the period $T = 20$ s and the amplitude $B = 0.2$ nT that accompanied the surface seismic wave at the distance 4600 km from the epicenter of the famous Good Friday Earthquake (also called the Great Alaska Earthquake) of Friday, March 27, 1964, with the magnitude $M = 8.5$. The epicenter was 20 km north of Prince William Sound. The method does not suppress magnetospheric disturbances. Moreover, in modular measurements, all information about the polarization of the oscillations is lost.

An approach that could be called the advanced interval method [15] (we mentioned this method in Section 2.5) is used to extract the magnetic signal in the near-field zone. The idea is that neither the vibrations of the sensors, which lead to seismographic noise, nor the relative movements of the elements of the measuring device, which lead to the microphone effect, emerges within the relatively short time interval from the beginning of the earthquake to the instant when the seismic wavefront arrives at the observation point. In contrast to modular measurements, here it is possible to determine the polarization of seismomagnetic oscillations. Using this approach, Belov, Migunov, and Sobolev were the first to record the magnetic signal from the source of the epicentral zone of the powerful Kamchatka Earthquake that occurred on December 25, 1972 (magnitude $M = 6$, depth 80 km, epicentral distance 70 km). In the 15-s interval before the first arrival of seismic waves, a fairly powerful ($B = 0.5$ nT) 9-s bipolar magnetic pulse was detected; the pulse was probably related to the formation of a large-scale rupture in the source. The abrupt leading front of the pulse appeared 4.5 s after the beginning of the earthquake and 10 s before the arrival of the seismic wave.

Clearly, a seismic wave generates not only a magnetic field but also an electric field. Measurements of the electric components are also hindered by the presence of noise. However, synchronous recording of the horizontal components of the electric and magnetic fields would make it possible, at least in principle, to suppress seismographic noise and discriminate the electric field associated with the seismic wave. Especially simple and promising are measurements of the electric-field component parallel to the Love wavefront. In this case, there is no seismographic noise (if the region is horizontally homogeneous). As regards magnetospheric noise, one may try to compensate it by using the data on the horizontal component of the variable magnetic field that is orthogonal to the Love wavefront and the data on the surface impedance at the observation point.

In addition to the discussed methods, there is the gradient method, based on measuring the difference signal from two spaced magnetic-field sensors in order to suppress magnetospheric noise [53]. The idea of this method is that the horizontal gradients of the field of magnetospheric waves may, generally speaking, be much smaller than the horizontal gradients of seismomagnetic waves. However, all information about the amplitude and polarization of the signal is lost in gradient measurements.

There is also the spectral-polarization method, used to suppress all types of noise in recording magnetic oscillations

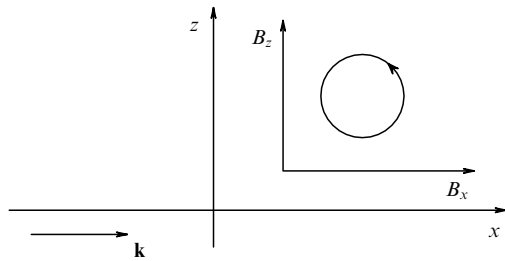


Figure 5. Polarization of seismomagnetic oscillations in the picture plane. The arrow shows the direction in which the seismic waves propagate.

in the teleseismic zone [28–30, 54–56]. The method is based on the a priori idea about the very special polarization state of the seismomagnetic field [25]. We introduce a Cartesian system of coordinates (x, y, z) such that the Earth's surface, which is assumed flat, coincides with the (x, y) plane and the z axis is directed vertically upward. We suppose that in the lower half-space ($z < 0$), which is assumed to be horizontally homogeneous, a planar elastic wave $\exp[i(kx - \omega t)]$ propagates in the positive direction of the x axis. We are interested in the magnetic field $\mathbf{B}(x, z, t)$ in the upper half-space ($z \geq 0$), where it satisfies two equations: $\nabla^2 \mathbf{B} = 0$ and $\nabla \mathbf{B} = 0$. For stimulated oscillations of the magnetic field, the dependence on x and t is the same as for the elastic wave, and the dependence on z is determined by the Laplace equation, the condition that the field be solenoidal, and the condition that the field decrease with increasing z :

$$\mathbf{B} = \frac{B}{\sqrt{2}}(1, 0, i) \exp[k(ix - z) - i\omega t]. \quad (29)$$

Thus, the theory predicts a definite and very special polarization state of the magnetic oscillations: the magnetic vector lies in the so-called picture plane, i.e., in the vertical plane orthogonal to the seismic wavefront. Next, if the mechanical vibrations are harmonic, magnetic oscillations are circularly polarized. Finally, the polarization of magnetic oscillations is left-hand, i.e., the tip of the magnetic vector rotating counterclockwise in the picture plane is viewed such that the seismic wave propagates from left to right (Fig. 5). These properties are of a general nature: they depend neither on the type of seismic wave nor on the specific mechanism by which the seismic wave energy is transformed into the magnetic field energy. The combination of these properties is used as a distinctive feature in detecting seismomagnetic signals against the background of noise by the spectral-polarization method.

Here is an example of how the spectral-polarization method was used to detect the magnetic field of a Love wave [23]. On November 29, 1998, an $M = 7.7$ earthquake occurred in Indonesia. A magnetometer and a seismograph were located in Siberia at the distance 6400 km from the epicenter. Figure 6 shows the seismogram of Love waves from this event. The coordinate system is oriented such that the z axis points upward and the x axis coincides with the tangent of the arc of the great circle that passes through the epicenter, in accordance with Fig. 5. The spectrum of mechanical vibrations in the interval from 14:35:41 to 14:38:41 UT exhibited a maximum at 23 mHz, while the spectrum of magnetic oscillations showed no such maximum at this frequency. Thus, neither a simple comparison of the oscillograms nor spectral analysis allows detecting a seismomag-

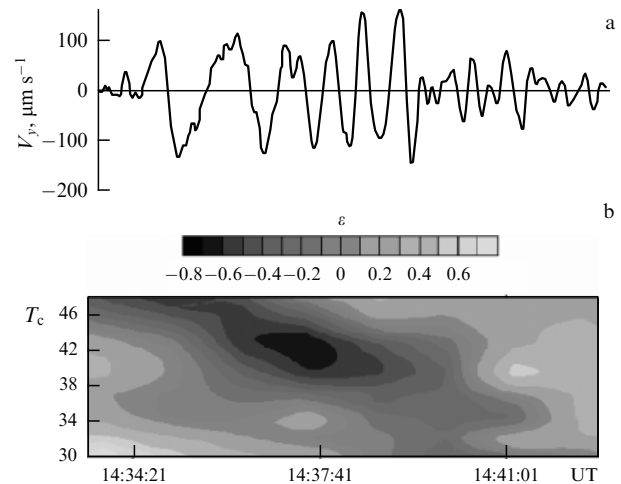


Figure 6. Comparison of seismic vibrations (a) with the polarogram of magnetic oscillations (b). Positive (negative) values of the parameter ε correspond to the rotation of the magnetic field clockwise (counterclockwise) in the vertical plane orthogonal to the seismic wavefront [23].

netic signal because of the high level of magnetospheric noise. Hence, the spectral-polarization filtration method was employed.

It has proved convenient to describe the polarization state of magnetic oscillations by the ellipticity ε , which varies from -1 to $+1$ and is chosen such that its positive (negative) values correspond to right-hand (left-hand) polarizations. Figure 6b shows the ellipticity ε as a function of the oscillation period T and time. Clearly, in accordance with what was to be expected, the range of negative values of ε approximately coincides with the central part of the Love wave packet. At 14:35:00 UT, the magnetic oscillations at the frequency 23 mHz have a left-hand and almost circular polarization ($\varepsilon = -0.8$). According to the data on ellipticity and on the spectrum of magnetic oscillations, the amplitude B can be estimated by the value of the circular component with left-hand direction of rotation of the magnetic vector. At 23 mHz, the value was found to be 0.01 nT. Dividing this value by the amplitude V of the Love wave, we obtain the estimate $\xi = B/V \sim 10^2$ nT m $^{-1}$ s. The parameter ξ is of special interest because it is independent of the amplitude of mechanical vibrations. It is assumed that in the future, the value of ξ will allow estimating the electrokinetic coefficient of rock in natural seams [29] (see Section 4.1).

Thus, the onset time, duration, frequency, and polarization of magnetic oscillations allow assuming that a magnetic field generated by a Love wave has actually been detected. This, however, is not enough, and the problem of detecting seismomagnetic signals cannot be considered solved. Systematic observations are needed to test the method in various geological conditions and build up a sampling large enough for statistical investigations.

Here is one more example. A very powerful earthquake ($M = 9.3$) occurred at 00:58:53 UT on December 26, 2004 in the Indian Ocean near the east coast of the northern part of Sumatra. Analysis of this event is in a certain sense exemplary, because it signifies that the complexity of detecting co-seismic magnetic oscillations, whose existence is predicted by theory, is connected solely with the presence of intense noise. Rayleigh and Love surface waves generated in the earthquake traveled around the world several times,

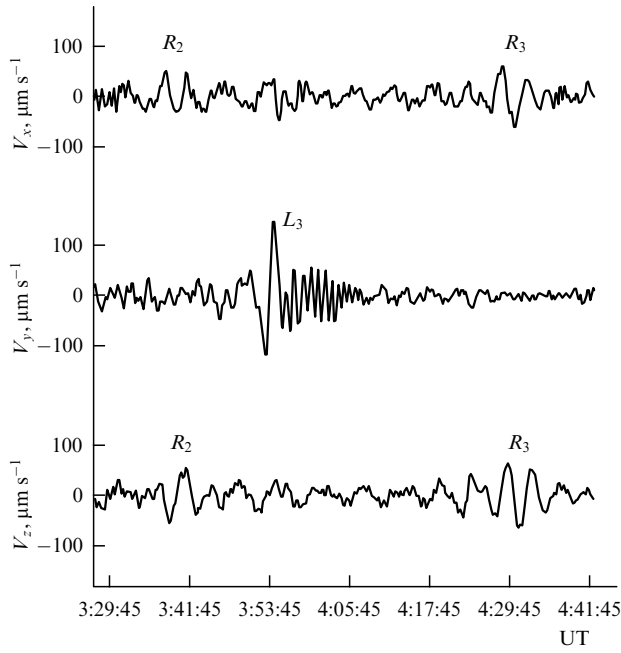


Figure 7. A seismogram taken at the Talaya Station (East Siberia) that demonstrates the presence of Rayleigh (R) and Love (L) waves after a strong earthquake on Sumatra [56]. The wave packet R_2 reached the station along the long arch of the great circle passing through the epicenter (the respective packet R_1 propagating along the short art of the great circle is not shown here). The packet R_3 is the round-the-world echo signal. Judging by the time of emergence, the packet L_3 is also an echo signal.

retaining a rather large amplitude (Fig. 7). This implies that observations at different points on the surface of the terrestrial globe can be used to detect a useful signal. Magnetic data gathered at the Mondy Observatory, located in the south of the Irkutsk region (Russia) on the Russian–Mongolian border and the Sodankylä Geophysical Observatory, located above the Arctic Circle in Finland, have been used to detect magnetic signals [56]. At both observatories, the signal was detected by the spectral-polarization method, although the distances to the epicenter were great (5390 and 8798 km).

3. Waves in the magnetosphere

Electromagnetic waves of extraterrestrial origin in the lower part of the ULF range were first detected in 1741 at the Uppsala Observatory. Celsius, the observatory director at the time, discovered them by simultaneously observing pulsations of the compass needle and pulsations of the northern lights. In the 19th century, ULF waves were observed by Nirvander in Helsinki and Stewart at the Kew Observatory near London. At the same time, the idea was put forward that magnetic-field oscillations are generated by varying currents in the ionized layers of the upper atmosphere. An interesting point (which proved to be extremely important much later) was the discovery of waves in the upper part of the ULF range (0.2–5 Hz). Waves in the 1-Hz range were detected by Sucksdorff [7] at the Sodankylä Geophysical Observatory and Harang [57] at the Tromse Observatory (Norway). In 2006, at the EGU General Assembly in Vienna, a special session titled ‘Pc1 Pearl Waves: Discovery, Morphology and Physics’ devoted to the 70th anniversary of this discovery was held [58].

For a long time, only empirical material was gathered, and only in the 1950s were the theoretical bases established for interpreting ULF waves in the framework of magnetohydrodynamics [59] and the general theory of propagation of electromagnetic waves in plasmas [60]. This was followed by a period of exhaustive comprehension of the facts, of the physical interpretation of the empirical laws established earlier, and of planning and implementing terrestrial and satellite observations in order to verify theoretical expectations. The main achievements along these lines have been thoroughly described in reviews and monographs [1, 41, 4, 6, 8, 11–14]. Research on waves in the magnetosphere continues. In this section, we discuss some of the new results and focus on applications of the theory of ponderomotive forces [61] to the theory of ULF waves (Sections 3.1–3.3) and on the interpretation of the dependence of the occurrence of Pc1 waves (known as ‘pearls’) on the number of sunspots (Sections 3.4 and 3.5).

3.1 Equatorial plasma condensation by ion-cyclotron waves

The fact that the energy density of ULF waves is comparable to the plasma pressure [6] speaks in favor of the idea of a noticeable redistribution of plasma in the magnetosphere initiated by ULF waves. We discuss the theory in [62], which predicts that ion-cyclotron waves in the Pc1 range (0.2–5 Hz) ‘congregate’ the plasma along the geomagnetic field lines in the direction toward the equator. As a result, for a very moderate wave intensity, a nonmonotonic density distribution is formed with a maximum at the equator (see also Refs [63–67]).

We consider the balance of forces acting in the longitudinal direction in relation to the geomagnetic field:

$$\nabla_{\parallel} p = \rho g_{\parallel} + f_{\parallel}, \quad (30)$$

where p and ρ are the plasma pressure and density, g_{\parallel} is the projection of the acceleration of gravity on the lines of the geomagnetic field \mathbf{B} , f_{\parallel} is the time-average of the longitudinal component of the ponderomotive force acting on the plasma, and $\nabla_{\parallel} = \mathbf{B} \nabla$. From the Pitaevskii formula [61], we find that

$$f_{\parallel} = \frac{1}{16\pi} \left[(\varepsilon_{\alpha\beta} - \delta_{\alpha\beta}) \nabla_{\parallel} E_{\alpha}^* E_{\beta} + E_{\alpha}^* E_{\beta} \frac{\partial \varepsilon_{\alpha\beta}}{\partial \mathbf{B}} \nabla_{\parallel} \mathbf{B} \right], \quad (31)$$

where $\varepsilon_{\alpha\beta}$ is the plasma permittivity tensor. The time-dependence of the electric field \mathbf{E} of the wave is $\exp(-i\omega t)$. We suppose that a traveling ion-cyclotron wave propagates exactly along the magnetic field. Then (31) can be written as

$$f_{\parallel} = \frac{1}{8\pi} \left[(n^2 - 1) \nabla_{\parallel} E^2 + E^2 \frac{\partial n^2}{\partial B} \nabla_{\parallel} B \right], \quad (32)$$

where n is the refractive index and E is the wave amplitude. In the geometric optics approximation, $E \propto \sqrt{B/n}$. This allows eliminating the derivative with respect to the wave amplitude B from (32). We assume that the plasma consists of electrons and ions of the same kind. We now use the well-known expression for n [68], take the fact that $n^2 \gg 1$ into account, and find the ponderomotive acceleration

$$A_{\parallel} = - \left(\frac{cE}{2B} \right)^2 \frac{\Omega}{\Omega - \omega} \left(\frac{\omega}{\Omega - \omega} \nabla_{\parallel} \ln B + \nabla_{\parallel} \ln \rho \right), \quad (33)$$

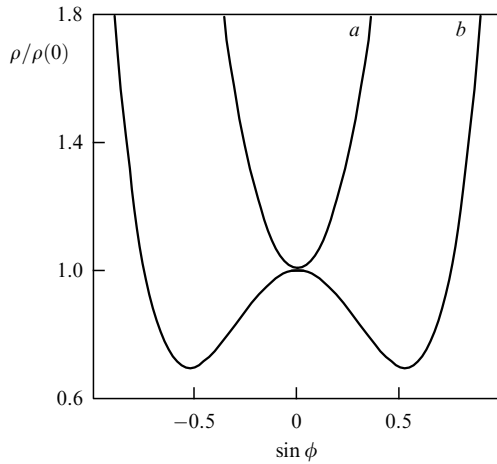


Figure 8. The shapes of the distributions of the plasma density along a geomagnetic field line [67]. Here, ϕ is the geomagnetic latitude. The curves a and b correspond to the subcritical and supercritical amplitudes of the ion-cyclotron wave.

where Ω is the ion gyrofrequency and ρ is the plasma density, with $A_{\parallel} = f_{\parallel}/\rho$.

With the equation of state $p = c_s^2 \rho$, where c_s is the speed of sound, we see that Eqn (30) becomes

$$\frac{c_s^2}{\rho} \frac{d\rho}{dz} = g_{\parallel}(z) + A_{\parallel}(z). \quad (34)$$

Here, we introduce the coordinate z along the wave trajectory, which by assumption coincides with the geomagnetic field line. Equation (34) should be supplemented with the relation

$$\frac{E(z)}{E(0)} = \left[\left(\frac{B(z)}{B(0)} \right)^3 \frac{\rho(0)}{\rho(z)} \frac{\Omega(z) - \omega}{\Omega(0) - \omega} \right]^{1/4}. \quad (35)$$

We assume that the point $z = 0$ coincides with a magnetic field minimum. In a dipolar magnetosphere, the minimum is located at the culmination point of the trajectory (on the equator).

Analysis of Eqns (33)–(35) shows that for $E(0) > E_c$, the plasma density distribution $\rho(z)$ has a maximum at $z = 0$. In a dipolar magnetosphere, the critical amplitude is given by [62]

$$E_c = \frac{2\sqrt{2}}{3c} \left(\frac{R_E g_E}{L} \right)^{1/2} \left[\left(\frac{\Omega_0}{\omega} \right)^{1/2} - \left(\frac{\omega}{\Omega_0} \right)^{1/2} \right] B_0, \quad (36)$$

where $R_E = 6371$ km is the Earth's radius, $g_E = 980$ cm s $^{-2}$ is the acceleration of gravity at the Earth's surface, and L is the McIlwain parameter, equal in our case to the distance from the center of the Earth to the apex of the magnetic field line in units of R_E . The quantities Ω_0 and B_0 are taken at $z = 0$. Figure 8 shows the plasma density distribution along a magnetic field line with $L = 5$ and $\omega/\Omega_0 = 0.5$ [67]. The value of the critical amplitude E_c is 0.58 mV m $^{-1}$. The curves a and b correspond to the subcritical ($E = 0.2$ mV m $^{-1}$) and supercritical ($E = 2$ mV m $^{-1}$) amplitudes of the ion-cyclotron waves. The range of applicability and the practical applications of the theory associated with the physics of ULF waves in the Pc1 range are discussed in Refs [63–66].

3.2 Acceleration of the polar wind by Alfvén waves

A characteristic feature of polar regions is the strong wind that carries the ionospheric plasma to the periphery of the magnetosphere [69, 70]. From the physical standpoint, polar winds are in many ways similar to solar wind [71]. The theory predicts a noticeable contribution of Alfvén waves to the acceleration of ions of the solar wind [72]. It is then only natural to assume that the same is true of ions in polar winds when Alfvén waves appear in an upward supersonic flow [73].

We use a simple model to show that the ponderomotive forces produced by waves in a flow increase the speed at the critical point and reduce the altitude of that point. Next, with certain reservations concerning the applicability of the model, we can say that in polar winds, the ponderomotive acceleration of the plasma increases downstream. (We recall that according to the classical solar wind theory [71], the acceleration decreases downstream.) Finally, the additional assumption that the wave field is transversely localized leads to the idea that thin long filaments with an increased speed and reduced plasma density form in the flow.

To describe the ponderomotive modification of polar winds caused by Alfvén waves, we use the Euler equation

$$u_i \nabla_{\parallel} u_i = -\frac{T}{m_i} \nabla_{\parallel} \ln N_i + \frac{e_i}{m_i} E_{\parallel} + g_{\parallel} + A_{\parallel}, \quad (37)$$

the continuity equation

$$\nabla_{\parallel} B^{-1} N_i u_i = 0, \quad (38)$$

and the quasineutrality condition

$$\sum e_i N_i = eN. \quad (39)$$

Here, u_i is the speed with which the ions move along the geomagnetic field lines, N_i is the ion concentration, with the subscript $i = 1, 2, \dots$ specifying the type of ion with a given ratio of charge e_i to mass m_i , N is the electron concentration, T is the plasma temperature, E_{\parallel} is the ambipolar electric field, and A_{\parallel} is the ponderomotive acceleration averaged over the wave period. It is assumed that $\max \{u_i\} \ll c_A$, where $c_A = (4\pi\rho)^{-1/2} B$ is the Alfvén velocity and $\rho = \sum m_i N_i$ is the plasma density. In what follows, we assume that all ions are positive and singly charged ($e_i = e$).

Ignoring the inertia of the electrons, we find that

$$E_{\parallel} = -\frac{T}{e} \nabla_{\parallel} \ln N. \quad (40)$$

Next, we account for the fact that the speed of the waves is much larger than the speed of plasma flow and ignore the Doppler effect in the expression for the ponderomotive acceleration:

$$A_{\parallel} = \left(\frac{c}{B} \right)^2 \left(\frac{1}{2} \nabla_{\parallel} E_{\perp}^2 - \frac{E_{\perp}^2}{B} \nabla_{\parallel} B \right), \quad (41)$$

where E_{\perp} is the amplitude of electric-field oscillations in the Alfvén wave. To match the structure of the wave field to the spatial ion distribution, which itself depends on this structure, we use the relation

$$\nabla_{\parallel} E_{\perp}^2 = E_{\perp}^2 \nabla_{\parallel} \ln \frac{B^2}{\sqrt{\rho}}, \quad (42)$$

valid for traveling Alfvén waves in the WKB approximation [38]. (See Ref. [74] regarding the problem of self-consistency in the case of standing waves.) After that, Eqn (37) can be written as [73]

$$u_i \nabla_{\parallel} u_i = -c_i^2 \nabla_{\parallel} \ln N N_i + G_{\parallel}, \quad (43)$$

where $c_i = (T/m_i)^{1/2}$ and $G_{\parallel} = A_{\parallel} + g_{\parallel}$, with

$$A_{\parallel} = -\left(\frac{cE_{\perp}}{2B}\right)^2 \nabla_{\parallel} \ln \rho. \quad (44)$$

The closed self-consistent system of equations (38), (39), (42)–(44) describes the ponderomotive redistribution of ions along the geomagnetic field lines caused by traveling Alfvén waves. We set $A_{\parallel} = \nabla_{\parallel} \phi$, with the ponderomotive potential

$$\phi = \left(\frac{cE_{\perp 0}}{B_0}\right)^2 \left(\frac{\rho_0}{4\rho}\right)^{1/2}, \quad (45)$$

and similarly $g_{\parallel} = \nabla_{\parallel} \varphi$. The gravitational potential is $\varphi = \kappa M_{\oplus}/r$, where κ is the gravitational constant, M_{\oplus} is the Earth's mass, and r is the geocentric distance. Here, $E_{\perp 0}$, B_0 , and ρ_0 are the values of the respective quantities at a certain point on the given field line. (For instance, this could be the point at which observations are made by a satellite.) With (38), we find the constants of motion

$$\frac{u_i^2}{2} + c_i^2 \ln N N_i - \psi = \text{const}, \quad (46)$$

$$B^{-1} N_i u_i = \text{const}, \quad (47)$$

which provide the solution of the problem in implicit form. Here, $\psi = \phi + \varphi$.

Analysis of Eqns (46) and (47) simplifies considerably in the static limit and in the case where the plasma consists of ions of one type. The static solution is of certain interest to magnetospheric physics. However, we must bear in mind that there is an anabatic wind blowing atop the polar cap, and this wind carries away the ionospheric plasma to the geomagnetic tail. Hence, we focus on the problem of a steady-state flow of a single-component plasma. The magnetic field lines above the polar cap are directed almost along the radius, and hence we can set $\nabla_{\parallel} = d/dr$. At this point in our discussion, it is convenient to introduce the dimensionless variables $z = r/r_0$, $w = u/u_0$, $s = c_s/u_0$, $\varepsilon = c_E/u_0$, and $\gamma = \kappa M_{\oplus}/r_0 u_0^2$. Here, $c_s = (2T/m_i)^{1/2}$, $c_E = cE_{\perp 0}/2B_0$, $u_0 = u(r_0)$, and $E_{\perp 0} = E_{\perp}(r_0)$, $B_0 = B(r_0)$. We write the Bernoulli equations using such variables as

$$\frac{w^2}{2} - s^2 \ln w - 2\varepsilon^2 w^{1/2} z^{3/2} = \frac{\gamma}{z} + 3s^2 \ln z + \text{const}. \quad (48)$$

The third term in the left-hand side accounts for the effect of ponderomotive forces on the flow.

We are interested in solutions of the Bernoulli equation that describe polar winds, i.e., monotonically increasing solutions $w(z)$ that pass through the critical point, $w_c(z_c)$. It is easy to verify that

$$z_c w_c^2 = \frac{\gamma}{3}, \quad w_c^2 - s^2 = \varepsilon^2 w_c^{1/2} z_c^{3/2}. \quad (49)$$

We now let r_0 coincide with the position of the critical point r_c . Then $z_c = 1$, $w_c = 1$, $\gamma = 3$, and $s^2 + \varepsilon^2 = 1$, with $0 \leq \varepsilon \leq 1$.

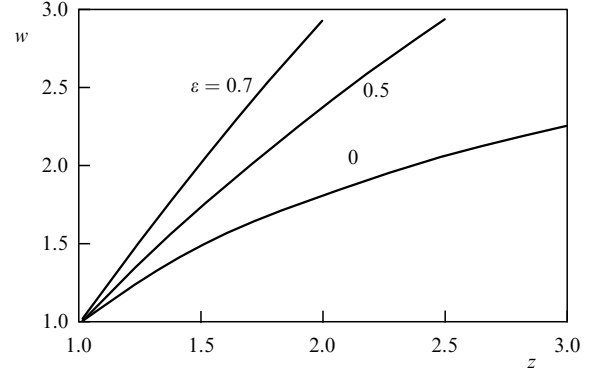


Figure 9. Dependence of the polar-wind speed on distance without waves ($\varepsilon = 0$) and with waves in the flow ($\varepsilon = 0.5$ and $\varepsilon = 0.7$). The variables in the figure are dimensionless.

Returning to the old notation, we obtain

$$u_c = (c_s^2 + c_E^2)^{1/2}, \quad r_c = \frac{\kappa M_{\oplus}}{3(c_s^2 + c_E^2)}. \quad (50)$$

We see that when traveling Alfvén waves ($c_E \neq 0$) occur in polar winds, the speed at the critical point increases and the altitude of this point decreases irrespective of whether the waves propagate to or away from the Earth's surface.

We next consider how Alfvén waves change the speed of polar winds above the critical point. We use the relation $s^2 + \varepsilon^2 = 1$ and, via the Bernoulli equation, we find the radial dependence of the speed, $w(z)$, in implicit form:

$$\begin{aligned} \frac{w^2}{2} - (1 - \varepsilon^2) \ln w - 2\varepsilon^2 \sqrt{w} z^{3/2} \\ = \frac{3}{z} + 3(1 - \varepsilon^2) \ln z - 2\varepsilon^2 - \frac{5}{2}. \end{aligned} \quad (51)$$

Figure 9 shows the functions $w(z)$ for different values of ε . We recall that $0 \leq \varepsilon \leq 1$. At $\varepsilon = 0$, there are now waves in the flow and the wind acceleration decreases as the distance to the Earth increases. Asymptotically, the acceleration $w dw/dz$ tends to zero like $1/z$ at $\varepsilon = 0$. Also interesting is the opposite limit, $\varepsilon = 1$. This case corresponds to cold winds induced by Alfvén waves [73]. In this case, the acceleration increases as the distance from the Earth increases: $w dw/dz \propto z$ [see Eqn (51) at $\varepsilon = 1$]. Clearly, in the real magnetosphere, the conditions needed for the theory to be valid are violated when z is large. In particular, as we move farther from the Earth, sooner or later the conditions that the ion velocity be small compared to the Alfvén velocity, the wave frequency be small compared to the ion gyrofrequency, etc. break down.

To complete the picture, we briefly discuss the transverse structure of polar winds. We suppose that a beam of Alfvén waves travels within a tube formed by magnetic field lines. The flow velocity u_{in} in this tube is higher than the velocity u_{out} in the main flow, while the plasma concentration N_{in} is lower than N_{out} . As we move farther away from the Earth, the contrast between u_{in} and u_{out} increases because u_{out} increases with the distance to the Earth logarithmically, while u_{in} increases in accordance with a power law (see Fig. 9). For the same reason, the well in the transverse distribution of plasma density becomes deeper. Thus, a reduced-density jet appears in the polar-wind flow. The drop $\Delta N = N_{\text{out}} - N_{\text{in}}$

can be estimated by the formula

$$\Delta N \sim \left(\frac{c_E}{c_s}\right)^2 N_{\text{out}}, \quad (52)$$

where $c_E = cE_{\perp}/2B$.

Deep and narrow troughs in the plasma density at the places where intense Alfvén waves are localized have been observed from the data provided by the Viking and Freja artificial Earth satellites (e.g., see Refs [75–77]). The picture that emerges allows understanding the origin of such troughs. Here is a specific example. Passing through the area of northern lights at the altitude 1500 km, the Freja satellite recorded in the Pc1 range transverse oscillations of the amplitude $E_{\perp} = 10^2 \text{ mV m}^{-1}$, with $B = 0.3 \text{ G}$ and $c_s = 2 \times 10^5 \text{ cm s}^{-1}$ [71], which by formula (52) yields $\Delta N \sim 0.7N_{\text{out}}$. This estimate agrees with the observational data.

3.3 Anharmonicity of Alfvén waves

The entire spectrum of the classical nonlinear effects can be observed in the magnetosphere: anharmonicity, combination frequencies, self-contraction of wave packets, self-focusing of wave beams, and many more [1, 4, 8, 14]. For instance, when averaged over the period, the quadratic-in-the-amplitude ponderomotive force of a standing Alfvén wave acts such that the plasma is pushed out of the nodes and gathers at the antinodes of the electric field. This results in specific anharmonicity effects in the oscillations [74]. In this connection, the following observation is of interest. The decrease in the density ρ between nodes and antinodes amounts to

$$\frac{\rho_{\text{max}}}{\rho_{\text{min}}} = \exp\left(\frac{Ec}{2Bc_s}\right)^2, \quad (53)$$

where E is the amplitude of electric field oscillations [78]. We see that for finite values of E and nearly zero values of the speed of sound c_s , an exponentially large plasma density perturbation emerges. This fact leads to a paradoxical conclusion that in the cold-plasma approximation ($c_s = 0$), the linear theory of standing Alfvén waves, which is widely used in the literature to calculate the spectrum of magnetohydrodynamic (MHD) oscillations in the magnetosphere, cannot be used in general.

In the magnetosphere, standing waves with nodes in the ionosphere are observed as what is known as Alfvén resonances, which are stimulated vibrations of the magnetic sheaths excited by external sources [79, 80]. In the Pc3 range (periods in the 10–45 s range), Alfvén resonances are generated by magnetoacoustic waves that penetrate the magnetosphere and originate in the interplanetary medium [13, 78], while in the Pc4 range (periods from 45 to 150 s) they are generated by Kelvin–Helmholtz surface waves traveling along the magnetopause [80]. By analogy with a nonlinear mechanical oscillator [81], we can assume that the anharmonicity that emerges as a result of a ponderomotive redistribution of the plasma between the nodes and antinodes of a standing wave should manifest itself in the dependence of the period T of the oscillations on the amplitude E , but this is not the case, because Alfvén resonances are not the natural oscillations of the magnetic sheaths. The oscillation spectrum is a continuous function of the parameter L given by the geocentric distance to the equator of the magnetic sheath in units of the Earth’s radius. We suppose that the magneto-

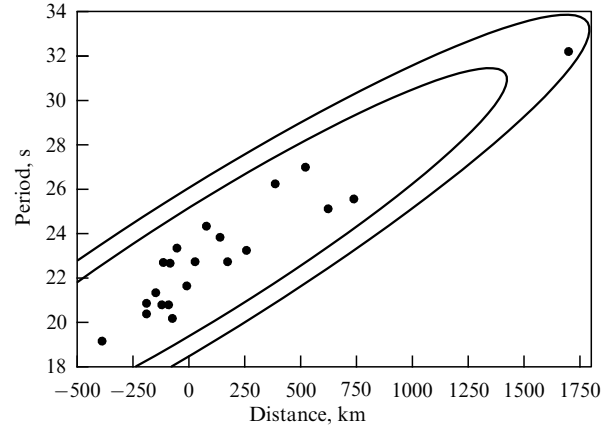


Figure 10. Dependence of the period of Pc3 oscillations on distance along the meridian to the oscillating magnetic sheath. The internal (external) ellipse limits the region within which a new experimental point will land with a 0.95 (0.99) probability.

sphere is subjected to an external force oscillation with the period T . In this case, the sheath with the parameter $L_{\text{res}}(T)$ resonates, and hence we have the relation

$$T \propto L_{\text{res}}^4 \sqrt{\rho} \quad (54)$$

linking T , L_{res} , and the plasma density ρ at the equator of the magnetic sheath [6, 82]. A ponderomotive perturbation of the plasma density is proportional to the intensity of the oscillations: $\delta\rho \propto E^2$ [74, 83]. With (54), we have

$$\frac{\delta L_{\text{res}}}{L_{\text{res}}} = -\left(8 + \frac{\partial \ln \rho}{\partial \ln L}\right)^{-1} \frac{\delta\rho}{\rho} \quad (55)$$

for a given period T of the driving force. Here, δL_{res} is the ponderomotive displacement of the resonating magnetic sheath. Thus, the specific feature of anharmonicity of standing Alfvén waves in the magnetosphere is that the position of the resonating magnetic sheath, determined by the parameter L_{res} , depends on the wave amplitude, but the period of the oscillations does not. Formally, this dependence can be represented as

$$L_{\text{res}}(T, E) = L_{\text{res}}(T, 0) (1 + \alpha E^2 + \dots), \quad (56)$$

where α is the nonlinearity of the standing Alfvén waves. It can be demonstrated that $\delta\rho < 0$ ($\delta\rho > 0$) if there is a node (antinode) of oscillations on the equator and, respectively, $\alpha > 0$ ($\alpha < 0$) if $|\partial \ln \rho / \partial \ln L| < 8$.

Series (56) was used in Ref. [78] in an attempt to detect the anharmonicity of oscillations of the magnetosphere from the data of terrestrial observation of Pc3 oscillations. Figure 10 shows the latitude dependence of the oscillation period T . The horizontal axis marks the distance x from the base point $x = 0$ (located on the geomagnetic latitude $\phi_0 = 44^\circ \text{ N}$) to the oscillating magnetic sheath. In the approximation of a dipolar magnetosphere, the parameter L_{res} can be expressed in terms of x as

$$L_{\text{res}} = \left(1 + 2 \frac{x}{R_E} \tan \phi_0\right) \cos^{-2} \phi_0. \quad (57)$$

We see in Fig. 10 that the period increases with the distance, as predicted by theory, with x and T related very strongly (the

correlation coefficient is 0.9), but the dependence of x on the amplitude H of the horizontal component of the magnetic-field oscillations is much weaker. And yet it was established through the use of statistical methods that $\partial x/\partial H$, which characterizes the anharmonicity of the oscillations, is nonzero with a high probability. In a three-hour measurement session, whose results are shown in Fig. 10, the oscillation amplitude randomly varied from 0.15 to 0.8 nT with the average value being 0.4 nT. A rough estimate produced $\partial x/\partial H \sim 300 \text{ km nT}^{-1}$.

To our knowledge, there have been no attempts to use artificial Earth satellites to detect the equatorial anomaly in the spatial distribution of plasma in the magnetosphere related to the generation of Alfvén resonances. And yet the theory irrevocably points to the possible existence of such an anomaly, even for moderate amplitudes of Pc3–4 oscillations. For example, we consider the fundamental harmonic of toroidal oscillations of the magnetosphere. In this case, the antinode of electric oscillations is located on the equator and we should therefore expect a maximum of the plasma density ρ if the amplitude of the oscillations exceeds a critical value [74]:

$$E > E_c \approx \frac{M_E g_E^{1/2}}{L^{7/2} R_E^{5/2} c}, \quad (58)$$

where M_E is the Earth's magnetic moment. For $L = 5$, we have a low threshold $E_c \approx 1 \text{ mV m}^{-1}$. It is surprising that to date the equatorial maximum in the plasma density has not been discovered in direct observations.

3.4 Ion-cyclotron resonator

Ion-cyclotron waves belong to the same branch of the dispersion curve as Alfvén waves [60, 68]. The existence of standing Alfvén waves, discussed in the previous section, has been proved by many observations in the magnetosphere made by satellites and at the Earth's surface by arrays of magnetometers (see, e.g., Refs [4, 6, 82]). Naturally, the question emerges whether ion-cyclotron waves exist. It is understandable that a traveling ion-cyclotron wave (there is no doubt that such waves exist in the magnetosphere; see Ref. [8]) can be represented by a linear combination of standing waves, but here we mean something quite different. What we have in mind is the existence of ion-cyclotron resonators. In this respect, there are so far only vague theoretical concepts, but still the problem merits attention. First, the model of an ion-cyclotron resonator exhibits interesting spectral properties. Second, the hypothesis [11, 85] that there are ion-cyclotron resonators in the equatorial zone of the magnetosphere naturally explains the 11-year high-degree modulation of the activity of Pc1 waves [58, 86].

To clarify the idea of an ion-cyclotron resonator, we recall the properties of the Alfvén branch of the dispersion curve. In a plasma containing several types of ions with different charge-to-mass ratios, this branch has zeros and poles of the square of the refractive index, n^2 . Between neighboring zero and pole, there is an opacity band. We suppose that the wave frequency is fixed, the wave propagates along the magnetic field, and its amplitude monotonically decreases in the direction of propagation. The sequences consisting of a pole, an opacity band, and a zero then alternate in space. Some time ago, it was assumed that because of wave reflection between a zero and a pole in n^2 , a resonator (cavity) forms, but this is not the case, because a pole absorbs waves completely. Reflection

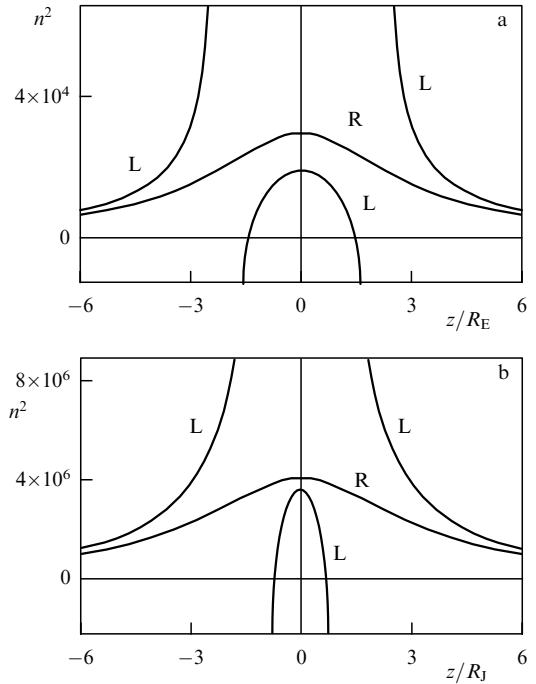


Figure 11. Square of the refractive index of waves of left-hand (L) and right-hand (R) circular polarizations along the lines of the dipole magnetic fields of the Earth (a) and Jupiter (b).

is possible only between two zeros, but there can be no adjacent zeros in a monotonically varying magnetic field. In the magnetosphere, this monotonic behavior breaks down near the equator, and an ion-cyclotron resonator may exist there [85]. Under certain conditions, two adjacent zeros of the refractive index may be located on two different sides of the equator, as shown in Fig. 11. The curves have been calculated with the McIlwain parameter equaling six. The coordinate z is measured from the magnetic-equator plane along a magnetic field line. The ion-cyclotron waves are left-hand (L) and the magnetoacoustic waves are right-hand (R) circularly polarized waves. Figure 11a corresponds to waves with the relative frequency $\omega/\Omega_{H^+} = 0.1$ in the terrestrial magnetosphere, with the following model of the plasma composition adopted: H^+ , 96%; He^+ , 2%; and O^+ , 2%; $N = 3.12 \text{ cm}^{-3}$. Figure 11b shows the dispersion curves for typical conditions in the Jovian magnetosphere at $\omega/\Omega_{H^+} = 0.0183$. The plasma composition is H^+ , 5%; O^+ , 70%; S^+ , 20%; and SO_2^+ , 5%; $N = 4000 \text{ cm}^{-3}$. In the one-dimensional model, the gap between the zeros of n^2 forms a high- Q resonator with a discrete spectrum of ion-cyclotron oscillations [84–86]. It is assumed that ion-cyclotron resonators are a characteristic feature of planets with an atmosphere and their own magnetic field. In the magnetospheres of Mercury and Venus, no ion-cyclotron resonators are formed, because Mercury has no atmosphere and Venus has no magnetic field.

We consider the wave equations

$$\frac{d^2 E_{\pm}}{dz^2} + k_{\pm}^2(z, \omega) E_{\pm} = 0, \quad (59)$$

which describe transverse electromagnetic waves within the flat-layered model with an external magnetic field that is perpendicular to the layers [60]. Here, $k_{\pm} = (\omega/c)n_{\pm}$ are the

wave numbers, $n_{\pm}^2 = \varepsilon_{xx} \pm \varepsilon_{yx}$ are the squares of the refractive indices for left-hand ($E_+ = E_x + iE_y$) and right-hand ($E_- = E_x - iE_y$) circular polarizations, and ε_{xx} and ε_{yx} are given by the well-known expressions for the components of the plasma permittivity tensor. In a small vicinity of the geomagnetic equator, the parabolic approximation of the geomagnetic field can be used. Next, for a two-component plasma at frequencies close to the so-called cutoff frequency ω_z , we can use the expansion

$$k_+^2(\omega) = \left(\frac{\partial k_+^2}{\partial \omega} \right)_{\omega=\omega_z} (\omega - \omega_z), \quad (60)$$

where $\omega_z = \Omega_2(1 + \eta)/(1 + \mu\eta)$, with $\mu = m_1e_2/m_2e_1$ and $\eta = \rho_2/\rho_1$, where $\rho_i = m_iN_i$, with N_i being the ion concentration. The light ions have $i = 1$ and the heavy ones have $i = 2$. At the cutoff frequency, $n_{\pm}^2 = 0$. (Note that the formula for the cutoff frequency is written for a dense plasma, with $\rho \gg B^2/4\pi c^2$, and $\rho = \rho_1 + \rho_2$. Some other limitations are described in Ref. [86].) Finally, it is convenient to introduce the dimensionless quantities

$$\zeta = \frac{z}{(2\eta)^{1/4}} \left[\frac{3\Omega_2(1 + \eta\mu)}{c_A R_E L(1 - \mu)} \right]^{1/2}, \quad (61)$$

$$\zeta_0 = (1 + \eta\mu)(2\eta)^{1/4} \left[\frac{R_E L(\omega - \omega_z)}{3c_A(1 + \eta)(1 - \mu)} \right]^{1/2},$$

with L being the McIlwain parameter. The quantities η , ω_z , Ω_2 , and c_A are taken at the minimum of the field $B(z)$. After that, Eqn (59) for E_+ becomes the Schrödinger equation for a linear harmonic oscillator,

$$\frac{d^2 E_+}{d\zeta^2} + [\zeta_0^2(\omega) - \zeta^2] E_+ = 0. \quad (62)$$

The solutions of Eqn (62) are known to be the parabolic cylinder functions

$$D_s(\sqrt{2}\zeta) = H_s(\zeta) \exp\left(-\frac{\zeta^2}{2}\right),$$

where $H_s(\zeta)$ is the Hermite polynomial and $s = (\zeta_0^2 - 1)/2$. If $E_+ \rightarrow 0$ as $\zeta \rightarrow \pm\infty$, then $s = 0, 1, 2, \dots$, and we obtain the equation $\zeta_0(\omega_s) = \sqrt{2s + 1}$, which describes the discrete spectrum of ion-cyclotron oscillations in the equatorial area of the magnetosphere. Recalling (61), we obtain

$$\omega_s = \frac{1 + \eta}{1 + \eta\mu} \left[\Omega_2 + \frac{3\sqrt{2\eta}(1 - \mu)c_A}{(1 + \eta\mu)R_E L} \left(s + \frac{1}{2} \right) \right], \quad s = 0, 1, 2, \dots \quad (63)$$

The condition that the field disappears at infinity requires special treatment in passing from Eqn (59) to Eqn (62). The resonator is located between two opacity bands, as shown in Fig. 11. Hence, the condition $E_+(\zeta \rightarrow \pm\infty) \rightarrow 0$, which leads to discrete spectrum (63), can be adopted only if each band is sufficiently wide. For this, the relative density of the heavy ions must be sufficiently high (see Ref. [86], where this condition and additional restrictions are discussed in detail in connection with the Earth's magnetosphere).

Spectrum (63) is equidistant, but estimates show that the interval between adjacent lines is much smaller than the frequency of the fundamental harmonic $s = 0$. The natural

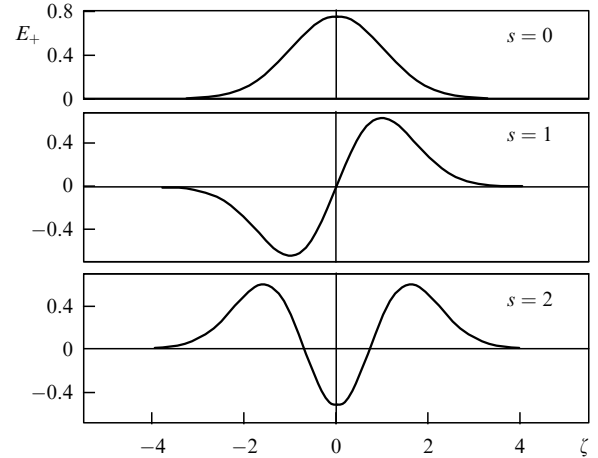


Figure 12. Eigenfunctions of an ion-cyclotron resonator. Here, s is the number of a harmonic. The dimensionless coordinate ζ is measured from the equatorial plane along a geomagnetic field line.

broadening of the spectral lines can be expected to lead to their merger. The eigenfunctions of the resonator corresponding to spectrum (63) are shown in Fig. 12, where we see that the field localization area depends on the number of the harmonic: the greater the number, the ‘thicker’ the resonator. The characteristic size of a resonator can be estimated as

$$\Delta z = 2\eta^{1/2} \left[\frac{c_A R_E L}{\Omega_2} \left(s + \frac{1}{2} \right) \right]^{1/2}. \quad (64)$$

According to these estimates, Δz for the first harmonics is much smaller than the length of the corresponding magnetic field line. In other words, the resonator is located in a narrow equatorial zone.

The ponderomotive force F_i acting on an ion of type i with charge e_i and mass m_i in the direction of a magnetic field line is given by

$$F_i = \frac{e_i^2 |E_+|^2}{4m_i \omega (\Omega_i - \omega)} \left(\frac{\partial}{\partial z} \ln |E_+|^2 - \frac{\Omega_i}{\Omega_i - \omega} \frac{\partial}{\partial z} \ln B \right). \quad (65)$$

As is known, in a single-component plasma, ω is always smaller than Ω_i and, hence, the sign of the first term in the right-hand side of (65), which determines the direction of what is known as the Miller force, is in this case independent of the frequency. In a multicomponent plasma, the situation is different. For instance, we suppose that the plasma consists of light ($i = 1$) and heavy ($i = 2$) ions with $m_1e_2 < m_2e_1$. The frequency of the ion-cyclotron wave may be either higher or lower than the gyrofrequency of the heavy ions. Accordingly, the directions of the forces acting on the light and heavy ions are either the same or the opposite. It is this last case that materializes in an ion-cyclotron resonator, where $\Omega_2 < \omega < \Omega_1$. This leads to ion separation in the field of the standing ion-cyclotron wave.

3.5 11-year activity variation in Pc1 waves

Pc1 waves have been observed in the form of periodic sequences of wave packets with the repetition period of 2 to 3 min. Within the standard model, this periodicity is explained by the fact that ion-cyclotron waves are excited in the outer radiation belt, travel to the Earth along geomagnetic field lines, are partially reflected by the ionosphere in

magnetically conjugate regions, and return to the radiation belt, transforming it into the self-excitation mode [1, 8, 11, 82]. According to theory, the repetition period τ is twice the time it takes a wave packet to travel from one conjugate region to the other.

Recently, there has been criticism of the standard model [87]. The main argument is that the data on the repetition period τ obtained from satellite data is the same as that obtained from terrestrial data, although it would seem that the first value should be half that of the second. In this connection, it was suggested [86] that a modification of the standard model is needed. Precisely, it was hypothesized that a wave packet oscillates in an ion-cyclotron resonator, being periodically reflected from the turning points located high above the ionosphere. Because a real resonator is open, a fraction of the packet energy is lost in the form of light to be observed on Earth as Pc1 waves. On a satellite, unless it is in the narrow equatorial zone, the observed wave packets have the same repetition period τ as on Earth. The ion-cyclotron resonator theory discussed in the previous section yields the following expression for τ :

$$\tau = \frac{\sqrt{2}\pi(1 + \eta\mu)^2}{3(1 + \eta)(1 - \mu)\eta^{1/2}} \frac{R_E L}{c_A} \quad (66)$$

We assume that $\mu = 1/16$ (a mixture of H^+ and O^+ ions), $\eta = 0.2$, $L = 5$, and $c_A = 7 \times 10^7 \text{ cm s}^{-1}$. We then have $\tau = 140 \text{ s}$, which is a typical value for the repetition period of Pc1.

The hypothesis that Pc1 waves are generated in an ion-cyclotron resonator solves another problem: the deep modulation of the frequency at which Pc1 waves appear, which is related to the 11-year cycle of solar activity. Prolonged observations have revealed that the activity of Pc1 waves is ten times less at the maximum of solar activity than at the minimum [88–90]. So far, there has been no conclusive interpretation of this dependence. How does the ion-cyclotron resonator theory explain it? First, we must bear in mind that at the minimum of the solar-activity cycle, the concentration of O^+ in the magnetosphere is much lower than at the maximum of the cycle, while the cyclic variation of the H^+ concentration is less pronounced [91, 92]. This means that Pc1 waves are observed most often in years when the relative concentration of oxygen ions along the paths of wave propagation is strongly reduced. Can we then assume, on these grounds, that the high-degree modulation of the Pc1 activity is simply the consequence of the 11-year variation in the width of the opacity bands? This is certainly an interesting assumption, but the alternative discussed in Ref. [58] appears to be more plausible.

We consider Fig. 13. The dispersion curves in Fig. 13a correspond to the case of a relatively high concentration of oxygen ions O^+ , as happens in years of maximum solar activity. Two zeros and two poles of the refractive index on the branch L are located symmetrically on both sides of the equator. Between the zeros and adjacent poles, there are the opacity bands. The branches L and R do not intersect. Figure 13b corresponds to the years of minimum solar activity, when the relative concentration of O^+ is low. The position of the poles on the L branch has not changed, but the zeros have shifted somewhat; however, if we are interested in the radical change in the general configuration, they are related to the fact that the L and R branches now intersect (black dots in Fig. 13b). Without going into details, we can

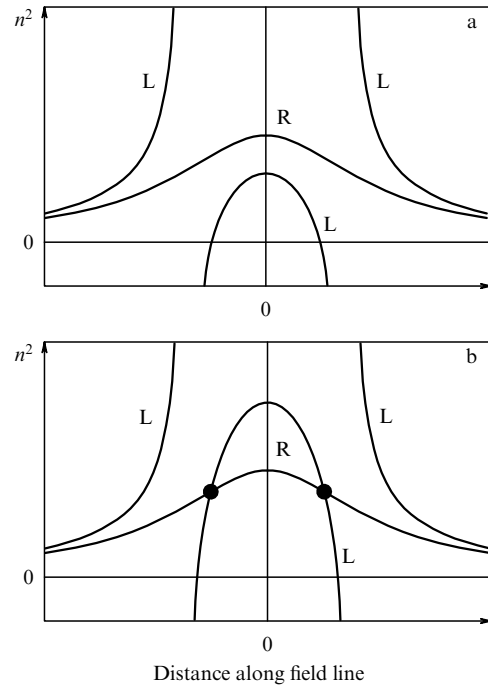


Figure 13. The topology of the dispersion curves in hydrogen–oxygen plasma (schematic depiction) in the cases of relatively high (a) and relatively low (b) oxygen concentration.

say that the intersection of the branches assists the linear transformation of L-waves into R-waves. The idea in Ref. [58] is that Pc1 waves are generated within a narrow zone near the equator in the form of L-waves and reach the Earth's surface in the form of R-waves if and only if the L and R branches intersect. It is understandable that the probability of the branches intersecting is higher at the minimum of the solar cycle than at its maximum.

Figure 14 depicts the plane of magnetospheric parameters [58, 86]. The top right part is occupied by the forbidden region, where the branches cannot intersect and waves from

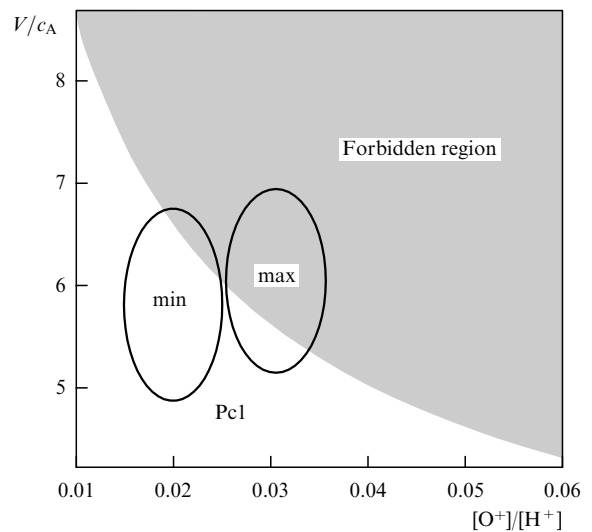


Figure 14. The plane of magnetospheric parameters: V is the speed of resonance protons responsible for the generation of Pc1 waves and $[O^+]$ and $[H^+]$ are the concentrations of oxygen and hydrogen ions. The left (right) ellipse schematically shows the typical state of the magnetosphere in the years of low (high) solar activity.

the generation region cannot reach the Earth's surface. Outside the forbidden region, the dispersion curves intersect, and the waves can reach the Earth's surface as a result of the partial transformation of L-waves into R-waves. The current state of the magnetosphere is described by a certain region in the plane of parameters. The location and configuration of such a region changes with time because of the natural variations in the magnetospheric parameters. The left and right ellipses in Fig. 14 schematically depict the typical states of the magnetosphere in the years of low and high solar activity. Clearly, the probability of a Pc1 wave emerging on the Earth's surface is proportional to the area of the lighter part of the ellipse and is higher at the minimum of solar activity than at the maximum.

4. Discussion

4.1 ULF waves and earthquakes

There are two areas of research in ULF waves generated in the Earth's crust. One is related to the search for and the physical interpretation of co-seismic electromagnetic signals. It is this area that we have discussed in the current review. The second area of research deals with the important but extremely difficult problem of short-term earthquake forecasting. After the catastrophic earthquake in Japan on January 17, 1995, an intensive search for electromagnetic precursors of earthquakes began within the large international projects Frontier/RIKEN and Frontier/NASDA under the general leadership of Hayakawa [93, 94]. Papers published in the period from 2002 to 2006 and devoted to this area of research can be found at <http://uec/japanese-activity/seismo-em>. Generally speaking, careful analysis of this problem merits a separate publication. Here we make only one remark.

The search for precursors has been extremely broad. Magnetometric arrays in seismically active regions have been built, observations are being perfected through the use of more sensitive recording devices, new mechanisms of precursor occurrence have been developed, and new methods of searching for precursors based on a combined approach to the problem with the use of terrestrial and extraterrestrial means are being investigated. The interest of the scientific community in this area of research is understandable. Significant achievements along these lines (e.g., building a magnetometric array along the Pacific coast, launching of specialized artificial Earth satellites, and constructing a magnetic gradiometer with the record-high sensitivity 1 fT m^{-1}) inspire hope that an effective earthquake forecasting service will be organized. However, many researchers are not very comfortable with the instability of the results of observation of electromagnetic signals that come before an earthquake. There have been many remarks in the literature that the complexity of the events that determine whether an earthquake occurs is the natural reason for such a situation. At the same time, the experimental research into the mechano-electromagnetic transformations that occur in the Earth's crust in much simpler conditions is scant. What we mean is the study of electromagnetic oscillations accompanying the propagation of seismic waves (see Section 2.3) and electromagnetic pulses that are generated in the source as a result of powerful movements of rock in the formation of a large-scale fault rupture (see Section 2.5). Research of this kind is not directly related to earthquake forecasting, but it could improve the understanding of the electrodynamic

processes that occur in the Earth's crust because as regards observing co-seismic electromagnetic oscillations, the way in which the field is excited is known, and only the mechanism of generation and spatial-temporal distribution of underground electric current remains undetermined and must be thoroughly studied.

There is another serious problem that has yet to be solved. Generation equation (6) contains at least five phenomenological parameters. (The number of parameters increases if the piezomagnetic properties of rock are described in greater detail than in deriving (6).) Usually, only a few 'typical' values of the parameters are selected, which yields only a rough estimate of the effectiveness of one mechanism or another. Interpreting real observational data requires, generally speaking, knowing the entire set of the parameters of the medium near the point of observation. Without achieving this, it is impossible to clarify the intricate picture of mechano-electromagnetic transformations, with the result that the involved search for seismomagnetic signals has, to a great extent, no meaning. Each observation of such signals attracts great attention because seismoelectrodynamics, just as any other geophysical theory, requires verification by practice. Mathematically, a formal solution of the general generation equation can easily be found for a given movement of the medium, but the merit of such a solution in interpreting an event is only marginal as long as the phenomenological parameters of the medium have not been specified. Inadequate attention to this problem is one of the reasons why electromagnetic signals from earthquakes have been discussed for more than a century (see, e.g., Refs [95, 96]), but still there is no agreement among geophysicists concerning the possibility of detecting such signals against the background of noise.

The experience of applying the methods of detection briefly discussed in Section 2.6 has proved that such signals can be detected. This opens up the possibility of using seismomagnetic observations to gain additional information about the structure and dynamics of the Earth's crust. The fairly simple and functional spectral-polarization method can be used in observations in the teleseismic zone. Of special interest are magnetic oscillations related to Love waves. Theoretically, Love waves trigger three physically different generation mechanisms, but only the magnetic field generated by the inertial mechanism reaches the Earth's surface. Such reasoning forms a basis for the method of seismomagnetic sounding of the Earth's crust, a method used to estimate the electrokinetic coefficient K , one of the most important transfer coefficients of rock [29]. Equation (1) contains two coefficients, the electric conductivity σ and the mechano-magnetic transformation α , which is proportional to K [33, 35]. Information about σ can be obtained by the standard magnetotelluric prospecting method. The idea of seismomagnetic sounding is that for a known value of σ , the interpretation parameter $\xi = B/V$ contains information about K . Here, B and V are the respective amplitudes of magnetic oscillations and mechanical vibrations. Usually, K is determined through laboratory measurements involving samples [97–99] or through theoretical estimates that use the well-known Helmholtz formula with allowance for the temperature and salinity of water, the structure and ratio of the porosity of rock, etc. In addition, it is usually advisable to be able to estimate the electrokinetic coefficient for rock of natural occurrence by measuring the magnetic field associated with a Love wave.

The unpredictability of the place and time of an earthquake occurring complicates the search for magnetic signals from the source. Only a few signals in the epicentral zone have been described in the literature. In all cases, the advanced interval method was used. We have mentioned the important observations during powerful earthquakes that were made earlier in Japan [21] and Kamchatka [15, 53]. At least one of these observations speaks in favor of the hypothesis that the inertial mechanism of generation in the source is predominant [23]. However, according to a recent report [100], there are no obvious traces of a seismomagnetic signal at the distance 210 km from the epicenter of a Sakhalin earthquake with the magnitude $M = 7.1$. There are reasons for concern here because the very possibility of recording seismomagnetic signals from the source and of using them for studying the processes of destruction in the Earth's crust is put to the test. Apparently, additional efforts and time are needed for building an empirical basis for verifying various hypotheses. The analysis of relatively weak earthquakes should be conducive to a faster accumulation of data. The experience of observations done in Caucasia on earthquakes with magnitudes $M = 2-4$ has shown that magnetic signals from weak earthquakes can be recorded by the gradient method at distances 50 to 100 km from the epicenter [101].

The above suggests that it is advisable to build a seismomagnetic testing ground [28] for carrying out special methodological experiments whose ultimate goal would be the measurement and comparative analysis of a set of parameters that determine the effectiveness of transforming mechanical energy into the electromagnetic field energy.

4.2 ULF waves of extramagnetospheric origin

An important factor that fuels the interest in the physics of ULF waves is the presence of difficult problems that require solution. We discuss one such problem now. It is related to the origin of Pc3 waves, mentioned in Section 3.3. These are quasimonochromatic waves with periods ranging from 10 to 45 s [1]. They are called permanent waves because they are observed almost continuously on the side of the Earth exposed to the Sun. Up to the 1970s, it was taken for granted that these waves are generated in the magnetosphere or at its boundary. This standpoint was stated, for instance, in reviews [11, 12] and in monograph [102]. Soon, however, the observational data gathered at the Borok Observatory of the Institute of Physics of the Earth, USSR Academy of Sciences, allowed establishing that the Pc3 waves are of extramagnetospheric origin, i.e., penetrate the magnetosphere from the interplanetary medium [6, 13]. At first, this result was considered by some to be controversial [82], but as time passed, the idea of the extramagnetospheric origin of Pc3 waves gained more and more support, stimulated numerous investigations, and was discussed in many publications (see the bibliography in Refs [1, 4]). The essence of the problem of Pc3 waves, which has yet to be solved, is discussed below. Here, we only note that decades after the problem was posed, some researchers continue to clarify the empirical rules discovered earlier without even attempting to solve the problem itself (e.g., see Refs [103, 104]).

To verify the idea of the extramagnetospheric origin of Pc3 waves, it was assumed that the frequency of the Pc3 waves at the Earth's surface and the frequency of MHD waves in front of the magnetosphere are the same if the Pc3 waves originate in the interplanetary medium and reach the Earth. For a number of reasons, not these two frequencies but the

frequency f of Pc3 waves at the Earth's surface and the magnitude B of the interplanetary magnetic field were actually compared. The correlations between f and B were studied, and the proportionality factor g was then carefully calculated by the formula

$$f = gB. \quad (67)$$

The correlation proved to be strong ($r = 0.78$), while the measured values $g = 5.8 \pm 0.3 \text{ mHz nT}^{-1}$ landed in the interval of theoretical estimates [13]. An important result of the research that followed was the convincing confirmation of the close link between f and B and the determination of g on the basis of new data gathered in terrestrial observations. It was found that g is very stable. Later, the value $g \approx 5.8 \text{ mHz nT}^{-1}$ was also obtained from a series of observations by space probes near Mercury, Venus, Earth, and Jupiter [105]. Thus, the coupling coefficient g is universal in the sense that it is relatively stable within an extremely broad range of the parameters of the flow of solar wind around the planets. In particular, the angle ψ between the interplanetary magnetic field and the direction of the solar wind varies from $\sim 20^\circ$ for Mercury to $\sim 80^\circ$ for Jupiter. According to all data from the known measurements, the spread in g does not exceed 10–20%.

But it seems that such a situation should not occur; this constitutes the problem. According to theory (see Refs [1, 13]), waves in front of the magnetosphere propagate along interplanetary magnetic field lines. The speed of the waves in the co-moving frame of reference is ten times lower than that of the solar wind in the reference frame related to the Earth. Hence, the terrestrial observer should discover a Doppler dependence of the type $g \propto |\cos \psi|$. But no such dependence was ever discovered. This striking inconsistency between predictions of theory and observational data suggests that the physics of a very common type of ULF wave is not fully understood. It must be acknowledged that as long as no answer to the question of why g is so stable under variations in ψ has been provided, theoretical estimates [13] will be only a source of guiding ideas in favor of the hypothesis of the extramagnetospheric origin of the Pc3 wave. If one corollary of the theory ($f \propto B$) agrees with the observational data but the other ($g \propto |\cos \psi|$) does not, the theory is either incomplete or wrong. However, the author believes that any new theory will also be based on the idea that Pc3 waves enter the magnetosphere from the interplanetary medium.

4.3 ULF waves and humans

Could it be that the appeal of ultra-low-frequency waves, of which we spoke in the introduction, stems from the special properties of their spatial-temporal structure? Could it be that these invisible and silent waves act on the subconscious in the same way as the rustling of leaves in a dense forest or ocean waves or the twinkling of stars has an effect on us? All living things on Earth in the course of millions of years have been subjected to constant, albeit weak, geoelectromagnetic oscillations. Questions of this kind emerge from time to time, and every person may have his or her opinion, but there is still no definite answer.

However, the interrelation between humans and ULF waves has more prosaic, but no less important aspects. There are indications that the geoelectromagnetic fields affect technological systems, especially long-distance communication lines. Lanzerotti [106] reported on a remarkable observa-

tion that telegraphists made in the 19th century: during a strong magnetic storm, the communications were disrupted but then came back to life even when the power sources were switched off. Moreover, spontaneous modulation of the telegraph operation mode was found to correlate with the northern lights, pulsing in the 3–30 mHz range, which in turn, as we now know, are closely related to ULF waves in the same range.

Varying geoelectromagnetic waves acting on long conductors, such as railroad rails, air ducts, gas and oil pipelines, casings of long cables, and overhead conductors, may be the cause of more serious problems. In extreme conditions, electromagnetic induction is capable of leading to extensive heating or even sparking in places with poor contacts, e.g., in flanges in poorly bolted joints or in corroded parts. All these factors can be successfully eliminated by employing special protection methods. But there is also another angle to this problem which does not bode well for the future. We speak of the stress that the environment experiences from the industrial and other activities of humans. In contrast to the general pollution of our environment, a weak and so far almost unnoticeable modification of the spectrum of geoelectromagnetic waves would not seem to merit any attention. But how well do we understand the role that natural electromagnetic phenomena play in the life of people and other living organisms? Much has been said about electromagnetic ecology, but does anybody know for sure about the mechanisms through which electromagnetic fields affect the body? It is believed that the necessary knowledge will come with time, but some researchers predict that it will be too late.

A quarter of a century ago, Fraser-Smith, speaking of the anthropogenic modification of ULF electromagnetic waves, expressed the general anxiety by stating that humankind already affects the global activity of ULF geomagnetic waves and that this threat will become only greater in time [107]. He based his reasoning, among other things, on reports on the relation between the activity of Pc1 waves and the operation of electronic and radio devices (e.g., see Refs [108–112]). Especially convincing evidence of the effect of human activity on Pc1 waves is presented by what is known as the ‘weekend effect,’ which amounts to the fact that the activity of Pc1 waves undergoes a one-week variation on average, with its maximum on Sunday.

Fraser-Smith discovered the weekend effect [108] by analysis based on the data on 12 years of continuous observation of Pc1 waves in the vicinity of San Francisco. The result needed independent verification because some researchers doubted that the weekend effect and other such effects were real [113, 114]. Such verification was carried out (see Ref. [115]) by using the data of the continuous recording of Pc1 waves in the course of 35 years at the Borok Observatory of the Institute of Physics of the Earth, Russian Academy of Sciences. The Pc1 waves were observed in a series that lasted on the average about an hour. From 1958 to 1992, 15,000 series of the overall duration 14,500 h were recorded.

To establish the seven-day variation in the presence of strong noise related to variations in solar activity, we used the method of synchronous detection with an accumulation step of one year. Figure 15 shows the results. The activity of Pc1 waves is characterized here by the duration of oscillations amounting to hours; to make the picture more graphic, we removed the linear trend when constructing the figure. There is a distinct maximum in the wave activity on Sunday. At the end of the 35-year period of accumulation, the absolute height

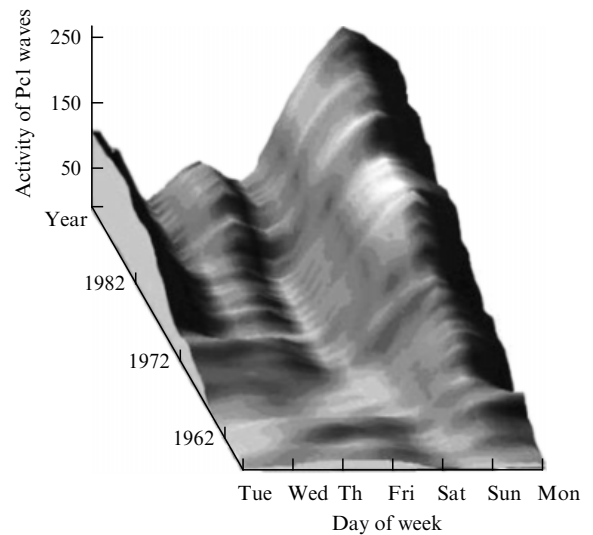


Figure 15. Evolution of the week cycle of activity of Pc1 waves (0.2–5 Hz) recorded at the Borok Observatory of the Institute of Physics of the Earth, Russian Academy of Sciences, in the period from 1958 to 1992 [115].

of the maximum was 2220 h. Thus, according to this figure, the span of the weekly variation in Pc1 activity amounts to 10–12%. It was also found [115] that in synchronous accumulation with a period of seven days, the rate of growth of the variation amplitude is considerably higher (this result is statistically reliable) than the rate of growth in accumulation with other periods (e.g., six or eight days).

Thus, there seems to be no doubt that the weekend effect exists and is related to human activity. But the mechanism of this relation is not known. Some researchers believe that the radiation emitted into the magnetosphere by high-power electric lines and/or the effect on the ionosphere of acoustic noise of industrial origin suppresses the activity of Pc1 waves on workdays, but these are no more than guesses.

5. Conclusion

The most important point discussed above is that the physics of ultra-low-frequency electromagnetic waves of natural origin continues to be a rapidly developing area of research. The problems associated with this area of research are enriched by interesting aspects, and these require solution, while the old problems are sometimes looked upon from a new angle. At the same time, as is the case with successfully developing areas of research, there is the tendency to avoid especially difficult questions, which in their time caused great interest, appeared to be extremely important, and were actively discussed by the scientific community, but were never solved. This is true of the question of the origin of Pc3 waves, the prevailing type of ULF waves, and the question of detecting seismomagnetic waves. The search for answers to such questions may lead to new ideas about the generation and propagation of ULF waves and about the relation of these waves to other geophysical phenomena. The prolonged existence of unresolved problems in this field of human endeavor is highly objectionable, because it is a challenge to our capability of understanding the physics of electromagnetic waves of natural origin.

The author expresses his deep gratitude to B V Dovbnaya, O D Zotov, J Kangas, B I Kline, R Lundin, A S Potapov, C Russel, M Hayakawa, and B Tsegmed for the fruitful

discussions of the problems associated with ULF waves. The work was supported by the Russian Foundation for Basic Research (Grant no. 06-05-64143).

References

- Guglielmi A V *MGD-Volny v Okolozemnoi Plazme* (MHD Waves in Circumterrestrial Plasma) (Moscow: Nauka, 1979)
- Weaver J T J. *Geophys. Res.* **70** 1921 (1965)
- Guglielmi A V "Some problems in seismo-electrodynamics: A review", in *Atmospheric and Ionospheric Electromagnetic Phenomena Associated with Earthquakes* (Ed. M Hayakawa) (Tokyo: TERRAPUB, 1999) p. 931
- Guglielmi A V, Pokhotelov O A *Geoelectromagnetic Waves* (Bristol: IOP Publ., 1996)
- Berdichevskii M N *Elektricheskaya Razvedka Metodom Magnitotelluricheskogo Profilirovaniya* (Electrical Prospecting with the Telluric Current Method) (Moscow: Nedra, 1968) [Translated into English of a related book (Golden: Colorado School of Mines, 1965)]
- Guglielmi A V, Troitskaya V A *Geomagnitnye Pul'satsii i Diagnostika Magnitosfery* (Geomagnetic Pulsations and Diagnostics of the Magnetosphere) (Moscow: Nauka, 1973)
- Sucksdorff E *Terr. Magn. Atm. Electr. (former J. Geophys. Res.)* **41** 337 (1936)
- Kangas J, Guglielmi A, Pokhotelov O *Space Sci. Rev.* **83** 435 (1998)
- Pititsyna N G et al. *Usp. Fiz. Nauk* **168** 767 (1998) [*Phys. Usp.* **41** 687 (1998)]
- Binhi V N, Savin A V *Usp. Fiz. Nauk* **173** 265 (2003) [*Phys. Usp.* **46** 259 (2003)]
- Troitskaya V A, Gul'el'mi A V *Space Sci. Rev.* **7** 689 (1967)
- Troitskaya V A, Guglielmi A V *Usp. Fiz. Nauk* **97** 453 (1969) [*Sov. Phys. Usp.* **12** 195 (1969)]
- Gul'el'mi A V *Space Sci. Rev.* **16** 331 (1974)
- Guglielmi A, Pokhotelov O *Space Sci. Rev.* **65** 5 (1995)
- Belov S V, Migunov N I, Sobolev G A *Geomagn. Aeron.* **14** 380 (1974)
- Sobolev G A *Osnovy Prognoza Zemletryaseniya* (Fundamentals of Earthquake Prediction) (Moscow: Nauka, 1993) [Translated into English (Moscow: Mir Publ., 1993)]
- Gershenson N I, Gokhberg M B, Yunga S L *Phys. Earth Planet. Interiors* **77** 13 (1993)
- Guglielmi A V, Levshenko V T *Dokl. Ross. Akad. Nauk* **329** 432 (1993)
- Guglielmi A V, Levshenko V T *Dokl. Ross. Akad. Nauk* **349** 676 (1996) [*Trans. (Dokl.) Russ. Acad. Sci. Earth. Sci. Sec.* **349** 1033 (1996)]
- Guglielmi A V, Levshenko V T *Izv. Ross. Akad. Nauk Ser. Fiz. Zemli* (9) 22 (1997) [*Izv., Phys. Solid Earth* **33** 712 (1997)]
- Iyemori T et al. *J. Geomagn. Geoelectr.* **48** 1059 (1996)
- Guglielmi A V, Levshenko V T, Ruban V F *Izv. Ross. Akad. Nauk Ser. Fiz. Zemli* (4) 91 (1999) [*Izv., Phys. Solid Earth* **35** 340 (1999)]
- Guglielmi A, Potapov A, Tsegmed B *Phys. Chem. Earth* **29** 453 (2004)
- Eleman F J. *Geomagn. Geoelectr.* **18** 43 (1966)
- Guglielmi A V *Geomagn. Aeron.* **26** 467 (1986)
- Guglielmi A V *Usp. Fiz. Nauk* **158** 605 (1989) [*Sov. Phys. Usp.* **32** 678 (1989)]
- Guglielmi A V, Ruban V F *Izv. Akad. Nauk SSSR Ser. Fiz. Zemli* (5) 47 (1990)
- Tsegmed B, Guglielmi A V, Potapov A S *Izv. Ross. Akad. Nauk Ser. Fiz. Zemli* (12) 41 (2000) [*Izv., Phys. Solid Earth* **36** 1021 (2000)]
- Guglielmi A V, Potapov A S, Tsegmed B *Izv. Ross. Akad. Nauk Ser. Fiz. Zemli* (3) 48 (2002) [*Izv., Phys. Solid Earth* **38** 218 (2002)]
- Guglielmi A V, Potapov A S, Tsegmed B *Ann. Geophys.* **47** 171 (2004)
- Guglielmi A V *Izv. Akad. Nauk SSSR Ser. Fiz. Zemli* (10) 109 (1992)
- Guglielmi A V *Phys. Scripta* **46** 433 (1992)
- Guglielmi A V *Dokl. Ross. Akad. Nauk* **343** 390 (1995)
- Landau L D, Lifshitz E M *Elektrodinamika Sploshnykh Sred* (Electrodynamics of Continuous Media) (Moscow: Nauka, 1982) [Translated into English (Oxford: Pergamon Press, 1984)]
- Sgrigna V et al. *Nuovo Cimento C* **27** 115 (2004)
- Ivanov A G *Izv. Akad. Nauk SSSR Ser. Geogr. Geofiz.* (5) 699 (1940)
- Frenkel Ya I *Izv. Akad. Nauk SSSR Ser. Geogr. Geofiz.* (4) 133 (1944)
- Alfvén H, Fälthammar C-G *Cosmic Electrodynamics* 2nd ed. (Oxford: Clarendon Press, 1963) [Translated into Russian (Moscow: Mir, 1967)]
- Keilis-Borok V I, Monin A S *Izv. Akad. Nauk SSSR Ser. Geofiz.* (11) 1529 (1959)
- Guglielmi A V *Izv. Akad. Nauk SSSR Ser. Fiz. Zemli* (7) 112 (1986)
- Guglielmi A V *Izv. Akad. Nauk SSSR Ser. Fiz. Zemli* (4) 53 (1991)
- Moiseev S S "Vmorozhennost' magnitnogo polya" ("Magnetic field freezing-in"), in *Fizicheskaya Entsiklopediya* (Physics Encyclopedia) Vol. 1 (Editor-in-Chief A M Prokhorov) (Moscow: Sovetskaya Entsiklopediya, 1988) p. 286
- Dorman L I "O vozmushchenii magnitnogo polya pri volnovykh i struinykh techeniyakh v provodyashchei srede" ("On perturbing of the magnetic field in wave and jet flows in a conducting medium"), in *Voprosy Magnitnoi Gidrodinamiki i Dinamiki Plazmy* (Aspects of Magnetic Hydrodynamics and Plasma Dynamics) Vol. II (Riga: Izd. AN LatvSSR, 1962) p. 63
- Guglielmi A V, Levshenko V T, Pokhotelov D O *Izv. Ross. Akad. Nauk Ser. Fiz. Zemli* (8) 18 (1996) [*Izv., Phys. Solid Earth* **32** 645 (1996)]
- Chelidze T L *Zh. Eksp. Teor. Fiz.* **87** 635 (1984) [*Sov. Phys. JETP* **60** 364 (1984)]
- Guglielmi A V *Izv. Ross. Akad. Nauk Ser. Fiz. Zemli* (4) 75 (2002) [*Izv., Phys. Solid Earth* **38** 317 (2002)]
- Landau L D, Lifshitz E M *Teoriya Uprugosti* (Theory of Elasticity) (Moscow: Nauka, 1987) [Translated into English (Oxford: Pergamon Press, 1986)]
- Gorbachev L P, Surkov V V *Magn. Gidrodinamika* **23** (2) 3 (1987) [*Magnetohydrodynamics* **23** 117 (1987)]
- Kasahara K *Earthquake Mechanics* (New York: Cambridge Univ. Press, 1981) [Translated into Russian (Moscow: Mir, 1985)]
- Brune J N *J. Geophys. Res.* **75** 4997 (1970)
- Shteinberg V V *Izv. Akad. Nauk SSSR Ser. Fiz. Zemli* (7) 49 (1983)
- Dobrovolskii I P *Teoriya Podgotovki Tektonicheskogo Zemletryaseniya* (Theory of Precursors of Tectonic Earthquakes) 2nd ed. (Moscow: Inst. Fiziki Zemli im O.Yu. Shmidta, 1991)
- Gokhberg M B, Krylov S M, Levshenko V T *Dokl. Akad. Nauk SSSR* **308** 62 (1989)
- Tsegmed B, Abstract of Ph.D. Thesis in Physics and Mathematics (Irkutsk: Institute of Solar and Terrestrial Physics, 2002)
- Guglielmi A et al. *Phys. Chem. Earth* **31** 299 (2006)
- Guglielmi A et al. *Izv. Ross. Akad. Nauk Ser. Fiz. Zemli* (11) 63 (2006) [*Izv., Phys. Solid Earth* **42** 921 (2006)]
- Harang L *Terr. Magn. Atm. Electr. (former J. Geophys. Res.)* **41** 329 (1936)
- Guglielmi A, Kangas J "Pc1 waves in the system of solar-terrestrial relations", in *ST4.6 Pc1 Pearl Waves: Discovery, Morphology and Physics* (Geophys. Res. Abstr., Vol. 8, Conveners J Kangas, A Guglielmi) (Vienna: EGU General Assembly, 2006) EGU06-A-00270
- Alfvén H *Cosmic Electrodynamics* (Oxford: Clarendon Press, 1950) [Translated into Russian (Moscow: IL, 1952)]
- Ginzburg V L *Rasprostraneniye Elektromagnitnykh Voln v Plazme* (Propagation of Electromagnetic Waves in Plasma) (Moscow: Fizmatgiz, 1960) [Translated into English (New York: Gordon and Breach, 1962)]
- Pitaevskii L P *Zh. Eksp. Teor. Fiz.* **39** 1450 (1960) [*Sov. Phys. JETP* **12** 1008 (1961)]
- Guglielmi A V *Izv. Akad. Nauk SSSR Ser. Fiz. Zemli* (7) 35 (1992)
- Guglielmi A V et al. *Astrophys. Space Sci.* **200** 91 (1993)
- Guglielmi A V et al. *J. Geophys. Res.* **100** 7997 (1995)
- Guglielmi A V, Pokhotelov O A, Feigin F Z *Izv. Vyssh. Uchebn. Zaved. Radiofiz.* **39** 464 (1996) [*Radiophys. Quantum Electron.* **39** 315 (1996)]
- Guglielmi A et al. *J. Geophys. Res.* **101** 21493 (1996)
- Guglielmi A et al. *Earth Planets Space* **51** 1297 (1999)
- Lifshitz E M, Pitaevskii L P *Fizicheskaya Kinetika* (Physical Kinetics) (Moscow: Nauka, 1979) [Translated into English (Oxford: Pergamon Press, 1981)]
- Banks P M, Holzer T E *J. Geophys. Res.* **74** 6317 (1969)

70. Schunk R W, Sojka J J *J. Geophys. Res.* **94** 8973 (1989)
71. Parker E N *Interplanetary Dynamical Processes* (New York: Wiley-Interscience, 1963)
72. Belcher J W *Astrophys. J.* **168** 509 (1971)
73. Guglielmi A, Lundin R *J. Geophys. Res.* **106** 13219 (2001)
74. Guglielmi A *J. Geophys. Res.* **102** 209 (1997)
75. Lundin R et al. *J. Geophys. Res.* **95** 5905 (1990)
76. Lundin R et al. *Geophys. Res. Lett.* **21** 1903 (1994)
77. Stasiewicz K et al. *J. Geophys. Res.* **102** 2565 (1997)
78. Guglielmi A, Lundin R “Anharmonicity of standing Alfvén waves in the magnetosphere” *Geophys. Res. Abst.* **6** 00594 (2004); SRef-ID: 1607-7962/gra/EGU04-A-00594
79. Hasegawa A, Chen L *Space Sci. Rev.* **16** 347 (1974)
80. Southwood D J *Space Sci. Rev.* **16** 413 (1974)
81. Landau L D, Lifshitz E M *Mekhanika* (Mechanics) (Moscow: Nauka, 1988) [Translated into English (Oxford: Pergamon Press, 1976)]
82. Nishida A *Geomagnetic Diagnosis of the Magnetosphere* (Berlin: Springer, 1978) [Translated into Russian (Moscow: Mir, 1980)]
83. Allan W J *Geophys. Res.* **98** 1409 (1993)
84. Guglielmi A V, Potapov A S, Russell C T *Pis'ma Zh. Eksp. Teor. Fiz.* **72** 432 (2000) [*JETP Lett.* **72** 298 (2000)]
85. Guglielmi A V *Dokl. Akad. Nauk SSSR* **174** 1076 (1967)
86. Guglielmi A, Kangas J, Potapov A *J. Geophys. Res.* **106** 25847 (2001)
87. Mursula K et al. *J. Geophys. Res.* **106** 29543 (2001)
88. Matveeva É T *Geomagn. Aeron.* **27** 392 (1987)
89. Mursula K et al. *J. Geophys. Res.* **96** 17651 (1991)
90. Kangas J et al. *Geophysica* (Geophys. Soc. Finland) **35** 23 (1999)
91. Young D T, Balsiger H, Geiss J J *Geophys. Res.* **87** 9077 (1982)
92. Stokholm M et al. *Ann. Geophys.* **7** 69 (1989)
93. Hayakawa M *Trans. IEE Jpn. A* **121** 893 (2001)
94. Hayakawa M “Editor’s note”, in *Japanese Activity in Seismo Electromagnetics: Publication List 2002–2006* (Ed. M Hayakawa) (Tokyo: Univ. of Electro-Com., 2007)
95. Orlov A P *Zemletryaseniya i Ikh Sootnosheniya s Drugimi Yavleniyami Prirody. Zametki po Povodu Zemletryaseniya 1887 Goda* (Earthquakes and Their Relation to Other Natural Phenomena: Notes on the Earthquake of 1887) (Kazan: Izd. Tip. V.M. Klyuchnikova, 1887)
96. Bauer L A *Terr. Mag.* **XI** 135 (1906)
97. Parkhomenko É I *Yavleniya Elektrizatsii v Gornykh Porodakh* (Electrization Phenomena in Rock) (Moscow: Nauka, 1968)
98. Avellaneda M, Torquato S *Phys. Fluids A* **3** 2529 (1991)
99. Jouniaux L, Pozzi J-P “Streaming potential measurements in laboratory”, in *Intern. Workshop on Seismo-Electromagnetics* (Tokyo: Univ. Electro-Communications, 1997) p. 85
100. Migunov N I, Sobolev G A *Izv. Ross. Akad. Nauk Ser. Fiz. Zemli* (3) **81** (2006) [*Izv., Phys. Solid Earth* **42** 256 (2006)]
101. Guglielmi A V, Levshenko V T *Izv. Ross. Akad. Nauk Ser. Fiz. Zemli* (5) **65** (1994)
102. Jacobs J A *Geomagnetic Micropulsations* (Berlin: Springer-Verlag, 1970)
103. Villante U et al. *Ann. Geophys.* **17** 490 (1999)
104. Villante U, Vellante M, de Sanctis G *Ann. Geophys.* **18** 1412 (2000)
105. Russell C T, Hoppe M M *Space Sci. Rev.* **34** 155 (1983)
106. Lanzerotti L J *J. Atmos. Terr. Phys.* **41** 787 (1979)
107. Fraser-Smith A C *Adv. Space Res.* **1** 455 (1981)
108. Fraser-Smith A C *J. Geophys. Res.* **84** 2089 (1979)
109. Gul’el’mi A V et al. *Geomagn. Aeron.* **18** 179 (1978) [*Geomagn. Aeron.* **18** 122 (1978)]
110. Zotov O D, Kalisher A L “Statisticheskii analiz effektivov iskusstvennogo vozdeistviya na ionosferu” (“Statistical analysis of human impact on the ionosphere”), in *Vozdeistvie Moshchnykh Radiovoln na Ionosferu* (Effect of High-Power Radio Waves on the Ionosphere) (Apatity: KO AN SSSR, 1979) p. 125
111. Samadani R, Fraser-Smith A C, Villard O G (Jr) *J. Geophys. Res.* **86** 9211 (1981)
112. Guglielmi A V, Zotov O D *Geomagn. Aeron.* **26** 870 (1986)
113. Menk F W *J. Atmos. Terr. Phys.* **47** 713 (1985)
114. Karinen A et al. *Ann. Geophys.* **20** 1137 (2002)
115. Guglielmi A, Zotov O “Human impact on the natural geophysical phenomena: Pc1 electromagnetic activity”, in *ST4.6 Pc1 Pearl Waves: Discovery, Morphology and Physics* (Geophys. Res. Abst., Vol. 8, Conveners J Kangas, A Guglielmi) (Vienna: EGU General Assembly, 2006) EGU06-A-01013